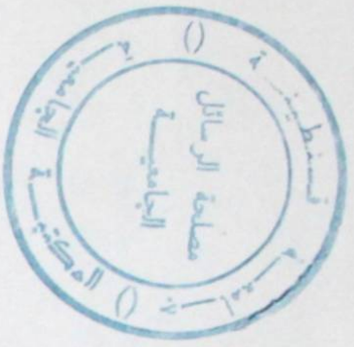

ROBUST CONTROL OF FLEXIBLE STRUCTURES

by

NASSIM M. ARBOUZ

B.S., Ecole Nationale Polytechnique, Algiers, 1982

M.S., University of Colorado at Boulder, 1985

A thesis submitted to the

Faculty of the Graduate School of the

University of Colorado in partial fulfillment

of the requirements for the degree of

Doctor of Philosophy

Department of Electrical and Computer Engineering

1989

This thesis for the Doctor of Philosophy degree by

Nassim M. Arbouz

has been approved for the

Department of

Electrical and Computer Engineering

by

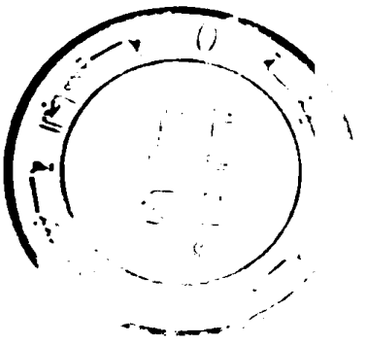

Renjeng Su

Henry Hermes

Date 11/29/88

Arbouz, Nassim M. (Ph.D., Electrical Engineering)

Robust Control of Flexible Structures

Thesis directed by Associate Professor Renjeng Su

The control of flexible mechanical systems has application to control of space systems, aircraft, robotics and active optics, to name a few. Structural mechanical systems are typically lightweight and highly flexible. These systems have distributed-parameter dynamics; their natural damping is very small; they have many densely packed low-frequency modes; and their model parameters are uncertain. Moreover, performance requirements such as pointing accuracy, shape control, and bandwidth are very stringent and make the problem of structural vibration more acute. Examples of flexible mechanical systems include a variety of space structures ranging from large antennas to very complex space stations. Another important application of flexible structural control is in robotics. The goal is to develop lighter and faster robots capable of moving larger payloads with low energy requirements.

In this dissertation, we first examined the single-input, single-output control of flexible structures. We established important time and frequency-domain properties that characterize elastic systems. Particularly, we demonstrated an interesting pattern of movement of the plant zeros as a function of the sensor location. This zero motion has a considerable implication on control design. We then presented a compensation method based on a frequency minimax technique, and uses a search procedure which always converges to the optimal controller.

We also proposed the concept of "generalized lead-lag compensation". This method is intended for the noncollocated control of flexible structures. A theorem giving necessary and sufficient conditions for the existence of such a stabilizing controller is proved, and a systematic design procedure is given.

We also investigated the multi-output control of flexible structures. An optimal sensor placement procedure, based on eigenstructure assignment, is developed for the robust control of elastic systems.

This dissertation is dedicated to my parents for their unfailing support and encouragement.

ACKNOWLEDGMENTS

I wish to express my sincere gratitude and appreciation to my dissertation advisor, Dr. Renjeng Su, for his invaluable assistance and guidance over the course of this research.

TABLE OF CONTENTS

CHAPTER I

INTRODUCTION

1.1 Introduction

The capability of placing large loads in space makes possible the construction and deployment of large space structures. These structures can range from large antennas to very complex space stations. They are intended for zero-gravity environment of space with minimal strength requirements; are large in some measure; and, of necessity, are to be deployed on orbit. Although, no such space structure has yet been deployed, these systems are primary future projects of the National Aeronautics Space Agency (NASA) and other organizations. Presently, some facilities are available for ground testing of space structures, such as Mini-Mast and Scole at NASA-Langley.

The first challenge in controlling a large flexible structure (LFS) is to describe the structure, as accurately as possible, by a dynamical model. Usually, for this purpose, numerical finite element techniques are used. The resulting approximate structural representation is of very high order, has very small natural damping, and has many densely packed low-frequency modes. The second challenge is to design an implementable low-order compensator to control the system. The design should be robust to accommodate significant modeling uncertainties and truncated high-frequency dynamics; it should also meet stringent requirements such as pointing accuracy, shape control, bandwidth requirements etc. Another difficulty arises from the limitations on zero-gravity ground testing of the actual LFS.

The topic of this dissertation is the control of flexible structures. Emphasis is placed on investigating important properties that characterize elastic systems, and on the development of low-order and robust compensation methods.

1.2 Literature survey

Numerous authors have investigated the dynamics and control of flexible structures. In what follows, we survey some of the work available in the literature.

The first step for any control design is to represent the system by a mathematical model. Flexible structures are distributed parameter systems, and therefore can theoretically be modeled with partial or integro-differential equations. However, this approach is impractical for all but simple structures. Instead, in most cases approximate finite representations can be obtained by finite element techniques.

Structural models for early space vehicles were based on two approaches: The equivalent beam models using Ritz or Galerkin method, or the lumped mass models connected with springs [2, 3]. These representations were quite accurate, since the early spacecrafts could be approximated as beams or cylinders with elastic modes of high frequency and weakly coupled.

Large flexible structures, currently being considered, are more complex and are analyzed with more sophisticated finite element techniques such as NASTRAN, SPAR etc. These special softwares feature large problem size capability, and run at the high speed of today's computers.

The accuracy of a finite element model is a function of the number of elements used in the model. In other words, the modeling details determine the complexity and size of the structural representation. Several examples dealing with the dynamics of LFS can be found [2, 4].

The second step of a control problem is to design a controller that meets the specified requirements and that has adequate robustness properties. For flexible structures, the finite element model (FEM) is only an approximate representation of the infinite dimensional system. In addition, it is usually too large for any practical design. Therefore, the FEM must be further truncated to a reduced-order design model (ROM). Consequently, the design has to cope with a high dimensionality, with sizable uncertainties in model parameters, and with the effect of the truncated dynamics.

In general, the truncation procedure is based on frequency and bandwidth considerations [1]. More sophisticated model reduction techniques are proposed [2]. For example, in [5] a procedure is given where the modes are selected according to the influence of the sensors and actuators.

There is quite an extensive literature in finite dimensional control theory for flexible structures. Clearly, no single approach is best for all cases. Given a design problem, it is up to the control engineer to choose among all the available tools. The choice should be based on the specifics of the problem, the performance requirements, hardware availability and so on.

One of the control approaches utilized is the classical pole placement method, which has been applied to several design examples [6]. Curtain [7] derived formulas which can give an a-priori estimate of the closed-loop poles.

Modal decoupling procedures in conjunction with modal filters are used in [8] to deal with the effect of the truncated dynamics (spillovers). Balas [16] also uses modal control and introduces additional terms ('innovations feedthrough') in the controller and estimator equations to decrease the sensitivity to spillover.

Optimal control theory has been extensively applied to LFS control. In [9], optimal control techniques are applied to reduced-order models, and a parameter

optimization is performed by solving a Lyapunov equation. Linear-quadratic-Gaussian (LQG) methodologies are also used to achieve a design insensitive to parameter variations. For instance, a case study is presented in [10], where the LQG approach with loop-transfer-recovery (LTR) is used to synthesize a robust fine-pointing control system for a large space antenna. Breakwell [11] combines the LQG procedure with modal decoupling to develop optimal slewing schemes for flexible spacecrafts. However, in most of these cases, plant uncertainties are not dealt with explicitly. This is mostly due to the lack of relationship between one's choice of weighting functions and robustness.

Identification and adaptive control have also been investigated to update the ROM via on-line parameter estimation and adaptation. In [12] a method is proposed based on the principle of least-squares, and in [13] an extended Kalman filter design procedure is presented. A model reference adaptive procedure that does not require explicit parameter identification has been applied by Kaufman [14] and Mufti [15] to the control of large structural systems. The method uses the model-following principle and Lyapunov stability theory; the system is also guaranteed to be stable if the sensors and actuators are collocated.

In this dissertation, we begin our study by investigating important frequency and time-domain properties of the plant describing an elastic system; this can provide a useful insight and a clear understanding of the control problem. We then develop low-order and robust compensation techniques for different classes of flexible structures.

1.3 Dissertation outline

In chapter II, we emphasize some important aspects specific to LFS control. We first discuss the problem of modeling elastic structures and, as an example, derive

an analytical model for a flexible beam in translational motion. We then address the sensor placement, the model reduction and the measurement spillover issues.

Chapter III deals with the single-input single-output (SISO) control of structural systems; and represents the core of this dissertation. We first examine an important frequency domain property; precisely, we show analytically the relationship between the sensor locations and the plant zeros for a class of structures. This effect has a considerable implication on control design. We then present a compensation technique for the SISO robust control design for flexible structures. The method is based on a frequency minimax approach, and uses a search procedure which always converges to the optimal stabilizing controller.

We then develop the concept of 'generalized lead-lag compensation'. This approach is especially intended for the case where the sensor and actuator cannot be exactly collocated. A theorem on the existence of such stabilizing controller is proved and a systematic design procedure is given.

In chapter IV, we consider a multi-output design and investigate the capabilities of multivariable control for flexible structures. An optimal sensor placement , based on eigenstructure assignment, is developed for the robust control of structural systems.

The conclusions of this dissertation and some directions for future research are included in chapter V.

1.4 Summary of contributions

1. We prove analytically, for a class of flexible systems, the effect of the sensor positioning on the loci of the plant zeros. This relationship between sensor placement and zero loci has a considerable importance for control design.

2. A search procedure for Kwakernaak's minimax control design is given. The scheme facilitates the numerical search and always converges to the stabilizing optimal controller.

3. We develop the concept of 'generalized lead-lag compensation'. The method is applicable to a class of dynamical systems which are characterized by a pattern of interlacing poles and zeros on the jω-axis. The approach provides robust low-order compensation for pole-zero patterns that are not easy to compensate for. A special yet important application is when there is a positional gap between the sensor and actuator.

4. We show how a multi-sensor design can enhance the robustness of the closed-loop system. Using known results in eigenstructure assignment, we derive an optimal sensor placement procedure for robust control of flexible structures.

CHAPTER II

SOME IMPORTANT ISSUES IN FLEXIBLE STRUCTURE CONTROL

Large flexible structures are characterized by a number of inherent properties that can lead to tremendous problems in control design; and at this time many questions are still open. In this chapter, we discuss some relevant issues in LFS control.

The first difficulty arises with the structural representation of LFS. It is a fact that performance requirements dictate how much modeling detail is needed, and accurate modeling is still based on experience and good judgement. Moreover, the theoretical model has to be experimentally verified by dynamic testing, which can be a major problem if full ground-testing is impossible.

Structural dynamic representations are merely simplified abstractions of the actual flexible structure. In addition, due to the very high dimensionality of the FEM, the control design must be performed on a truncated ROM. For complex systems, the order of the ROM itself can be very large. Due to the approximations involved, it is clear that significant uncertainties in the design model are bound to occur. In other words, the fundamental issues in LFS control are high dimensionality and plant uncertainties. Moreover, the LFS may have many low-frequency modes that are closely packed and are within the controller bandwidth. These modes have also very small damping factors ($< 0.1\%$). Another difficulty that must be overcome involves the activity of the unmodeled dynamics (spillovers). These residuals can alter both stability and performance.

One interesting aspect of elastic systems is the model dependency on the placement of the sensors and actuators on the structure. This dependency has profound implications on control design, as will be seen in the subsequent chapters.

2.1 Modeling

Flexible structures are distributed parameter systems and are typically combinations of trusses, panels and so on interconnected by joints. The elementary parts can be accurately modeled by partial differential equations (PDE) for strings, beams, membranes and other elementary flexible structures. But, large interconnected structures are usually too complex to be represented by PDE's. Even when it is possible, design techniques are not currently available for dealing with such infinite dimensional systems. Control theory of distributed parameter systems [17] is still at an early stage of development. However, by using finite element techniques, it is possible to obtain approximate models of finite dimension.

Consider a given physical elastic structure, and let w(t, x) represent the distributed displacement, off the equilibrium point, of a point x at time t. The finite element method is based on approximating w(t, x) by a finite modal expansion of the form

$$w(t, x) = \sum_{i=1}^{k} \phi_i(x)\, q_i(t) \tag{2.1}$$

where ϕ_i are said to be the mode shapes; q_i the mode amplitudes; and k can be very large, but finite. Then, a finite element model (FEM) of the following form may be established

$$M \ddot{q} + K q = F u \tag{2.2}$$

where M is a (k x k) mass matrix, K is a (k x k) stiffness matrix, q is a k-vector of mode amplitudes, F is a (k x ℓ) control influence matrix, and u is an ℓ-dimensional control vector. System (2.2) can be obtained by eigenfunction expansions (if PDE model is available) or by analyses with Nastran-type codes. Typically, for a large structure, the dynamical representation (2.2) consists of hundreds of ordinary differential equations.

Let Φ be the modal matrix whose columns are the structural mode shapes and so that

$$\Phi^t M \Phi = I$$

and

$$\Phi^t K \Phi = \Lambda^2 = \text{diag}(\omega_1^2, \ldots, \omega_k^2)$$

where, ω_i is the ith modal frequency. An equivalent modal model is then obtained as

$$\ddot{\eta} + \Lambda^2 \eta = \Phi^t F u \tag{2.3}$$

where

$$\eta = \Phi^{-1} q$$

is the modal vector.

Next, to illustrate, we consider a flexible beam system and derive an analytical dynamical model.

2.1.1 Flexible beam example

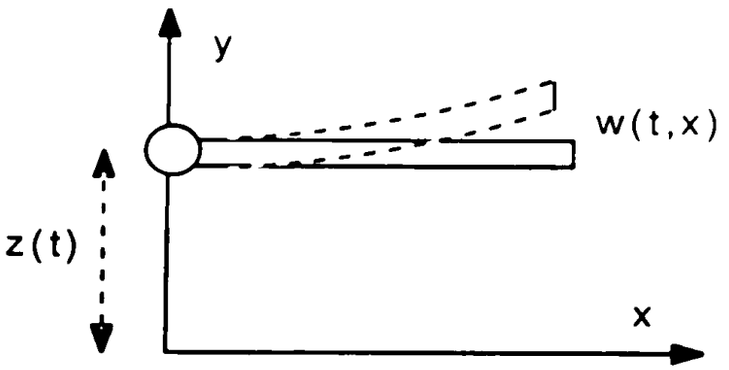

Fig. 2.1 Flexible beam in translational motion.

The beam, as depicted in Fig. 2.1, moves in the x-y plane and is of length L. At the end x = 0, the beam is clamped to an actuator with input force f(t) so that the beam translates in the y-direction. Let z(t) be the displacement y at x = 0, w(t, x) be the beam flexure from y = z(t), and v(t, x) = z(t) + w(t, x). This configuration amounts to the following boundary conditions on w(t, x)

$$w(t, 0) = w_x(t, 0) = w_{xx}(t, L) = w_{xxx}(t, L) = 0. \tag{2.4}$$

Let $\rho(x)$ be the mass density of the beam, and EI(x) be the bending rigidity. The kinetic energy is given by

$$T(t) = \frac{1}{2}\int_0^L \rho(x) \left(\frac{\partial v}{\partial t}\right)^2 dt\,. \tag{2.5}$$

Assuming that only bending contributes to the potential energy V(t), we have

$$V(t) = \frac{1}{2}\int_0^L EI(x) \left(\frac{\partial^2 w}{\partial x^2}\right)^2 dx\,. \tag{2.6}$$

To derive an equation of motion for the beam, we apply the Hamiltonian principle, ie.

$$\delta \int_{t_0}^{t_1} (T - V + W)\, dt = 0 \tag{2.7}$$

where (t_0, t_1) si any time interval, and W is the nonconserved work given by

$$\delta W(t) = f(t)\, \delta z(t). \tag{2.8}$$

Suppose the virtual displacement $\delta v(t)$ satisfies

$$\delta v(t_0) = \delta v(t_1). \tag{2.9}$$

Hence, after integration by parts, the variation of kinetic energy is given by

$$\delta \int_{t_0}^{t_1} T(t)\, dt = - \int_{t_0}^{t_1} \int_0^L \rho \left(\frac{\partial^2 v}{\partial t^2}\right) \delta v\, dx\, dt\,. \tag{2.10}$$

To compute the variation of potential energy, recall the boundary conditions (2.4). Therefore, we only consider the variations $\delta w(t, x)$ such that

$$\delta w(t, 0) = (\delta w)_x(t, 0) = 0$$

it then follows

$$\delta \int_{t_0}^{t_1} V(t)\, dt = \int_{t_0}^{t_1} \int_0^L \frac{\partial^2}{\partial x^2}(EI(x)\, w_{xx})\, \delta w\, dx\, dt \tag{2.11}$$

substituting (2.8), (2.10) and (2.11) in (2.7), and since $v(t, x) = w(t, x) + z(t)$, we obtain

$$\int_{t_0}^{t_1} [\int_0^L \rho(\frac{d^2 z}{dt^2} + \frac{\partial^2 w}{\partial t^2}) dx - f(t)]\, \delta z(t)\, dt +$$

$$\int_{t_0}^{t_1} \int_0^L [\, \rho(\frac{d^2 z}{dt^2} + \frac{\partial^2 w}{\partial t^2}) + \frac{\partial^2}{\partial x^2}(EI(x)\, w_{xx})]\, \delta w\, dx\, dt = 0\,. \tag{2.12}$$

The virtual displacements $\delta z(t)$ and $\delta w(t, x)$ are arbitrary, except for satisfying a few regularity conditions. It follows from (2.12) that

$$\int_0^L \rho(x) \left(\frac{d^2 z}{dt^2} + \frac{\partial^2 w}{\partial t^2} \right) dx - f(t) = 0 \tag{2.13}$$

and

$$\rho(x) \left(\frac{d^2 z}{dt^2} + \frac{\partial^2 w}{\partial t^2} \right) + \frac{\partial^2}{\partial x^2} \left(EI(x)\, w_{xx} \right) = 0 \tag{2.14}$$

Equations (2.13), (2.14) together with boundary conditions (2.4) describe the motion of the moving beam as shown in Fig. 2.1. Moreover, equation (2.13) describes how the actuating force f(t) affects the rigid-body motion of the beam. Due to the elasticity of the beam, the rigid body mode excites the structural vibrations. This relationship is modeled in equation (2.14).

The dynamics of the beam can be discretized by the following eigenexpansion, for which the solution of the PDE is assumed to be

$$w(t,x) = \sum_{i=1}^{\infty} \phi_i(x)\, q_i(t) \tag{2.15}$$

where $\{q_i\}$ are the mode amplitudes and $\{\phi_i\}$ is a set of orthogonal mode shapes that are solutions of the eigenproblem

$$\frac{d^4 \phi_i(x)}{dx^4} = k_i^4 \phi_i(x) \tag{2.16}$$

with boundary conditions (2.4). The well-known solutions have a closed-form expression

$$\phi_i(x) = (\cosh k_i x - \cos k_i x) - \frac{\cosh k_i L + \cos k_i L}{\sinh k_i L + \sin k_i L} (\sinh k_i x - \sin k_i x) \qquad (2.17)$$

where k_i satisfy

$$\cos k_i L \cosh k_i L + 1 = 0. \qquad (2.18)$$

In particular, $k_1 = 1.87$, $k_2 = 4.69$, $k_3 = 7.85$, ..., and $k_i \sim (2i - 1)\pi/2$ when i is large.

Suppose uniform mass density and bending rigidity. Let

$$\omega_i = k_i^2 \left(\frac{EI}{\rho}\right)^{\frac{1}{2}} \qquad (2.19)$$

and define a vector θ as

$$\theta = (z, q_1, q_2, \ldots)^t.$$

An infinite dimensional model can be obtained as

$$M\ddot{\theta} + K\theta = F f(t) \qquad (2.20)$$

where

$$M = \begin{bmatrix} 1 & \Phi_1 & \Phi_2 & \cdots \\ \Phi_1 & 1 & & \\ \Phi_2 & & 1 & \\ \vdots & & & \ddots \end{bmatrix}, \qquad K = \begin{bmatrix} 0 & 0 & 0 & \cdots \\ 0 & \omega_1^2 & & \\ 0 & & \omega_2^2 & \\ \vdots & & & \ddots \end{bmatrix},$$

$$F = [\,1\ 0\ 0\ \ldots]^t, \text{ and } \Phi_i = \frac{1}{L}\int_0^L \phi_i(x)\,dx. \qquad (2.21)$$

Note that zero-damping is assumed in the modeling which results in an infinite number of poles on the jω-axis, and that (2.20) can represent a class of flexible systems controlled by a single actuator.

2.2 Sensor placement problem

An interesting property of elastic structures is the model dependency on the spatial locations of the sensors and actuators on the structure. In this dissertation, emphasis is put on the sensor placement problem, and related questions are investigated. Since, for physical systems it is more practical to relocate sensors than actuators.

Suppose the displacements and velocities are measured by m point sensors, so that the output measurement y is

$$y = [y_1 \cdots y_m]^t = \tilde{C}_k \tilde{x}_k \tag{2.22}$$

where $\tilde{x}_k$ is a state vector defined by

$$\tilde{x}_k = [\, q_1 \dot{q}_1 \cdots q_k \dot{q}_k \,]^t \tag{2.23}$$

and

$$y_i = a_i w(x_i, t) + b_i w_t(x_i, t); \quad i = 1, \ldots, m \tag{2.24}$$

here x_i is the sensor location, a_i and b_i are constant real numbers. Therefore, the output matrix $\tilde{C}_k$ has the form

$$\tilde{C}_k =$$

$$\begin{bmatrix} a_1\phi_1(x_1) & 0 & a_1\phi_2(x_1) & 0 & \cdots & a_1\phi_k(x_1) & 0 \\ 0 & b_1\phi_1(x_1) & 0 & b_1\phi_2(x_1) & \cdots & 0 & b_1\phi_k(x_1) \\ \vdots & & & & & & \\ a_m\phi_1(x_m) & 0 & a_m\phi_2(x_m) & 0 & \cdots & a_m\phi_k(x_m) & o \\ 0 & b_m\phi_1(x_m) & 0 & b_m\phi_2(x_m) & \cdots & 0 & b_m\phi_k(x_m) \end{bmatrix}$$

(2.25)

It is obvious from (2.25) that $\tilde{C}_k$ is function of the sensor locations (x_1, ..., x_m), which indicates that the plant transfer function or the state-variable representation can be manipulated by varying the sensor positioning. In chapter III we show the effect of these variations on control design, and in chapter IV we use this model dependency to derive an optimal sensor placement for robust control.

2.3 Reduced-order model and robustness

The fundamental problem in flexible structure control is that the LFS is an infinite dimensional system to be controlled by a finite low-order compensator. As mentioned previously, the LFS is described by an approximate FEM of very high-order. Generally, the modeling errors for finite element representations tend to augment substantially with increasing modal frequencies. Moreover, the dimension of the FEM (k) is too large for control application, and a reduced-order design model (ROM) is sought. Evidently, the ROM can be subject to sizable parameter variations. For flexible structures, the principal plant uncertainties can be classified as follows.

a) Variations in the parameters of the design plant, due to the different approximations assumed in the modeling, approximate knowledge of physical parameters and so on.

b) Variations in the sensor (and actuator) positioning. It will be shown that these changes result in a movement of the plant zeros, and consequently have a direct effect on the system robustness.

c) Effect of the unmodeled high-frequency dynamics or spillovers, which can destabilize the closed-loop system. In the next subsection, we address the spillover question in more details.

2.4 Spillover effect

Consider the modal representation (2.3), and define a state-vector x_k as

$$x_k = (\eta_1 \dot{\eta}_1 \ldots \eta_k \dot{\eta}_k)^t.$$

Thus, the FEM model can be written in state-variable form as

$$\dot{x}_k = A_k x_k + B_k u \tag{2.26}$$

where A_k is (2k x 2k), B_k is (2k x ℓ) and are obtained from (2.2). For m point sensors, the output measurement y is

$$y = C_k x_k$$

where C_k is (m x 2k) and can be derived from (2.25).

Suppose a feedback controller is designed based on a ROM of low-frequency modes and of order n < 2k. Therefore, a residual system of order r = 2k - n remains, and has a direct effect on the closed-loop performance. Indeed, the residual modes are excited by the controls, giving rise to 'control spillover' which can degrade the

response. These residual modes are also measured and fed back to the system. This is a more serious problem that can cause unstability. More specifically, consider a state-space controller design for a flexible structure.

2.4.1 State-space design

Suppose a state-feedback observer type of controller is designed for a LFS. Let the n-dimensional ROM be

$$\dot{x}_n = A\,x_n + B\,u$$
$$y_n = C\,x_n \tag{2.27}$$

where A is (n x n), B is (n x ℓ), C is (m x n), x_n is the controlled state-vector and u is the control input. The r-dimensional uncontrolled residual system is

$$\dot{x}_r = A_r x_r + B_r u$$
$$y_r = C_r x_r \tag{2.28}$$

where A_r is (r x r), B_r is (r x ℓ), C_r is (m x r), x_r is the residual state-vector; and with the appropriate partition

$$A_k = \begin{bmatrix} A & 0 \\ 0 & A_r \end{bmatrix}, \qquad B_k = \begin{bmatrix} B \\ B_r \end{bmatrix}$$

$$C_k = [\,C \;\; C_r\,].$$

The feedback control law, based on the ROM, is given by

$$u = -\,K_n \hat{x}_n \tag{2.29}$$

where K_n is the state feedback which can be obtained by pole placement or optimal time-domain methods. The state vector $\hat{x}_n$ is estimated by the asymptotic observer

$$\dot{\hat{x}}_n = A\,\hat{x}_n + B\,u + L\,(y - C\,\hat{x}_n) \tag{2.30}$$

where L is the (n x m) observer gain matrix, with $m \leq n$. Of course, it is assumed that (2.27) is controllable and observable. Notice that the estimated state $\hat{x}_n$ is also function of the residual state x_r.

Define a measurement error by

$$e_n = \hat{x}_n - x_n \tag{2.31}$$

thus, an augmented system representing the overall dynamics can be defined as

$$\begin{bmatrix} \dot{x}_n \\ \dot{x}_r \\ \dot{e}_n \end{bmatrix} = \begin{bmatrix} A - BK_n & 0 & -BK_n \\ -B_rK_n & A_r & -B_rK_n \\ 0 & L_nC_r & A - L_nC \end{bmatrix} \begin{bmatrix} x_n \\ x_r \\ e_n \end{bmatrix}. \tag{2.32}$$

Equations (2.32) describes the dynamics of the closed-loop compensated system, including the uncontrolled residual modes. The term B_rK_n is called the 'control spillover' [1], which excites the residual system. Whereas, L_nC_r is the 'measurement spillover' which feeds back the residuals and can destabilize the closed-loop design.

Flexible structures, in general, have an inherent small damping which tends to increase at high frequencies. Hence the matrix A_r of high frequency modes, by itself, can be considered to be asymptotically stable. Moreover if the observation spillover L_nC_r is zero, by the separation principle, the augmented system (2.32) would remain stable. However, if it is nonzero, stability is not guaranteed. The following theorem gives a necessary and sufficient condition for the augmented system (2.32) to remain stable in the presence of measurement spillover.

Theorem 2.1

Suppose a state-variable controller/observer is designed for the ROM (A,B,C). Let

$$A_1 = \begin{bmatrix} A - BK_n & 0 & -BK_n \\ -B_r K_n & A_r & -B_r K_n \\ 0 & 0 & A - L_n C \end{bmatrix}, \quad A_2 = \begin{bmatrix} 0 & 0 & 0 \\ 0 & 0 & 0 \\ 0 & L_n C_r & 0 \end{bmatrix} \tag{2.33}$$

then, there exists a matrix P positive definite, and a matrix Q semi-positive definite such that

$$A_1^t P + P A_1 = -Q \tag{2.34}$$

and the augmented system (2.32) is asymptotically stable if and only if the matrix $(Q - 2PA_2)$ is positive semi-definite.

Proof

Let $X = (x_n\, x_r\, e_n)^t$ so that (2.32) can be written as

$$\dot{X} = A_1 X + A_2 X \tag{2.35}$$

with A_1 and A_2 as given by (2.33).

Assume (A,B,C) is controllable and observable. Then, there exist gain matrices K_n and L_n such that $(A - BK_n)$ and $(A - L_nC)$ are asymptotically stable. In addition, due to the inherent damping, the matrix A_r is asymptotically stable. Hence, A_1 is also stable and there exists a Lyapunov function $V(X) = X^tPX > 0$, where P is positive definite and satisfies

$$A_1^t P + P A_1 = -Q \tag{2.36}$$

with Q being positive semi-definite. The time-derivative of V(X) is

$$\dot{V} = \dot{X}^t PX + X^t P\dot{X}. \tag{2.37}$$

By substituting (2.35) into (2.37), we obtain

$$\dot{V} = X^t(-Q + 2PA_2)X \tag{2.38}$$

ie., $V(X) = X^tPX$ is a Lyapunov function for system (2.35) if and only if $(Q - 2PA_2)$ is positive semi-definite, which concludes the proof.

From the above theorem, we derive the following result which gives a direct relationship between the positive definite matrix P and the spillover term L_nC_r.

Theorem 2.2

A sufficient condition for system (2.32) to be asymptotically stable is

$$\|L_n C_r\|_f \leq \frac{1}{2\|P\|_f} \dagger \tag{2.39}$$

where P is the unique solution of

$$A_1^t P + PA_1 = -I. \tag{2.40}$$

Proof

Consider the derivative of V(X) as given by (2.38). Rayleigh's inequality states that

$$X^tQX \leq \lambda_{min}(Q)\, X^tX \tag{2.41}$$

in addition,

---

† The f-norm of a matrix $A = (a_{ij})$ is $\|A\|_f = \left(\sum_{j=1}^{n}\sum_{i=1}^{n}|a_{ij}|^2\right)^{1/2}$.

$$2X^tPA_2X \le 2|(X^tP)(A_2X)| \le 2\|P^tX\|_2 \|A_2X\|_2 \quad ††$$
$$\le 2\|P\|_2 \|A_2\|_2 X^tX. \tag{2.42}$$

Substituting the above inequalities in (2.38), shows that $\dot{V} \le 0$ if

$$\|A_2\|_2 \le \frac{\lambda_{min}(Q)}{2\|P\|_2}. \tag{2.43}$$

By choosing Q = I (identity) and taking the Frobenious norm, condition (2.43) becomes

$$\|L_n C_r\|_f \le \frac{1}{2\|P\|_f} \tag{2.44}$$

which concludes the proof.

Condition (2.39) of theorem (2.2) indicates that there is some upper limit on the observer gains for the closed-loop system to remain stable. A similar result in the frequency-domain can be established.

2.4.2 Frequency-domain design

Suppose the FEM of a flexible structure has an input-output transfer function P. Let C_n be a stabilizing compensator for a reduced-order plant P_n, which consists of n low-frequency modes (n < k). Then, P can be written as

$$P = P_n + P_r$$

where P_r is the plant of the remaining higher frequency modes. The residual P_r can be viewed as an additive perturbation in a unity feedback configuration as depicted in Fig. 2.2, and the subsequent theorem holds

---

†† The 2-norm of a matrix A = (a_{ij}) is (maximum eigenvalue of $A^t A)^{1/2}$.

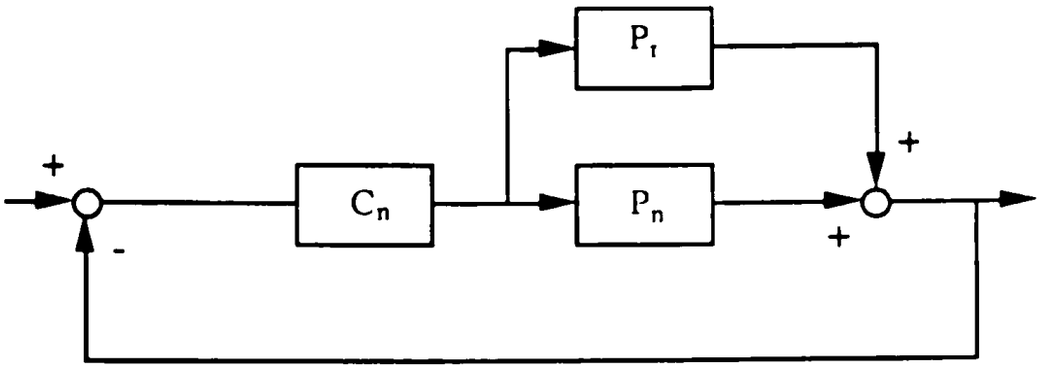

Fig. 2.2 Unity-feedback compensated system

Theorem 2.3

A sufficient condition for the closed-loop system of Fig. 2.2 to be stable is

$$\| C_n(\omega) \|_f \left\| (I+P_nC_n(\omega))^{-1} \right\|_f < \frac{1}{\| P_r(\omega) \|_f}. \tag{2.45}$$

Furthermore, if $\|P_nC_n(\omega)\|_2 << 1$ (at high frequencies), a sufficient condition for stability becomes

$$\| C_n(\omega) \|_f < \frac{1}{\| P_r(\omega) \|_f}. \tag{2.46}$$

Proof

Since C_n is a stabilizing compensator, then $(I+P_nC_n)^{-1}$ is stable. Moreover, the residual P_r consists of higher frequency modes which have some inherent damping, ie. P_r is stable. It then follows directly from [19] that the configuration of Fig. 2.2 is stable if

$$\| C_n(\omega) \|_2 \| P_r(\omega) \|_2 < \frac{1}{\left\| (I+P_nC_n(\omega))^{-1} \right\|_2} \tag{2.47}$$

ie., (2.45) is a sufficient condition for stability. Furthermore, the controller C_n has a

limited bandwidth, therefore $\|P_n C_n(\omega)\|_2 << 1$ at high frequencies and (2.46) follows directly.

The inequality (2.46) simply states that the compensator should roll-off rapidly at high frequencies to ensure a stable design. This also justifies the fact that if the controller bandwidth is properly limited, the high-frequency dynamics of the structure can be truncated for control design purposes.

CHAPTER III

SISO CONTROL OF FLEXIBLE STRUCTURES

This chapter considers the control of single-input single-output (SISO) flexible systems. The SISO case is investigated because of its practical importance, and because it can provide a basis for the development of multi-input multi-output (MIMO) control design methodologies.

We first give a systematic treatment of an important frequency-domain property of the plant describing a flexible structure. Precisely, we consider a class of flexible beams controlled by a single pair of actuator and position sensor, and show the relationship between sensor placement and the loci of plant zeros. This dependency of the plant zeros on the sensor location has a considerable implication on control design.

Then, we present a method for the robust control of a class of flexible structures. The method uses a frequency-domain minimax approach to robust compensation design. We also show a search procedure which always converges to the optimal stable solution. This is accomplished by parametrizing the set of all stabilizing controllers.

In the last section we give a controller design technique for a class of systems which are characterized by negligible structural damping and a pattern of interlacing poles and zeros. The goal is to achieve robust low-order compensation for high-order plants. The technique, based on the root-locus method, is a generalization of the classical lead-lag compensation. A theorem on the existence of such a stabilizing

controller is proved and a systematic design procedure is given. A special application of this approach is when the exact collocation of the sensor and actuator is not feasible.

3.1 A frequency-domain property: The loci of plant zeros

In the previous chapter, the relationship between the model and the sensor placement was discussed. In this section we start by clarifying this dependency of the dynamic model on the sensor/actuator positioning. Then, we consider a class of flexible beams, and show analytically an interesting pattern of loci of the plant zeros, as the sensor location varies along the beam.

Consider the modal representation (2.3) of a flexible structure. The dynamic equation for η_i $i = 1, ..., k$ can be written as

$$\ddot{\eta}_i + \omega_i^2 \eta_i = a_i u \tag{3.1}$$

where the row-vector a_i is function of the location of the actuators with respect to the ith mode shape.

Suppose the output y is measured by one position sensor. Hence, y can be approximated by

$$y = \sum_{i=1}^{k} r_i q_i(t) \tag{3.2}$$

where r_i depends on the sensor location with respect to the ith mode-shape. Thus, in the SISO case, the input-output transfer function is given by

$$P = \frac{y}{u} = \sum_{i=1}^{k} \frac{r_i a_i}{s^2 + \omega_i^2} \tag{3.3}$$

It is clear that all the poles of (3.3) lie on the imaginary axis and are invariant,

while the plant zeros are function of the placement of the actuator and the sensor. This frequency-domain property implies that some sensor/actuator locations may lead to more involved control problems than others. It is well-known that if the sensor is collocated with the actuator, the poles and zeros of (3.3) are interlaced in a regular pattern [20] on the imaginary axis, as depicted in Fig. 3.1. With this collocated arrangement, a simple lead compensator can stabilize all the modes, even though the response may not be satisfactory. This result, however, does not hold in a noncollocated situation. Actually, in this case, classical compensation techniques are not very effective.

3.1.1 Zero loci for flexible beams

Consider the class of flexible beams described by (2.20), and suppose the output y is measured by a position sensor located at x_j, ie.

$$y = C\theta \tag{3.4}$$

where

$$C = [\, 1 \;\; \phi_1(x_j) \;\; \phi_2(x_j) \;\; \ldots] \tag{3.5}$$

is the infinite-dimensional output vector.

Recall that zero damping is assumed in the dynamic model. For actual flexible structures, however, not all the poles have zero damping. The damping is negligible for a finite number of low-frequency modes, but becomes significant at high frequencies. For control purposes, it is usually possible to truncate those high-frequency modes that are adequately damped, as long as the controller bandwidth is properly limited. After such a truncation, a finite dimensional model (of order n) is

$$M\ddot{\theta} + K\theta = F f(t)$$
$$y = C\theta \tag{3.6}$$

where M, K, F and C are finite versions of the corresponding matrices in (2.20) and (3.5). Thus, the input-output transfer function of (3.6) can be written as

$$P = y/f = C(s^2 M + K)^{-1} F. \tag{3.7}$$

It is clear from (3.5), that the zeros of the transfer function (3.7) depend on the sensor location x_j. Now, we examine the effect of the sensor placement on the loci of the plant zeros. But, first we state the well-known fact that the plant P with a collocated sensor and actuator has the regular interlacing pattern of Fig. 3.1.

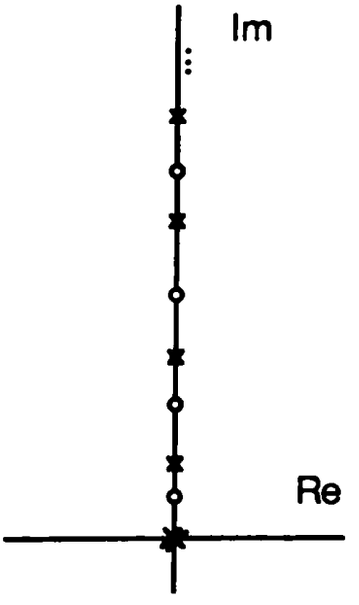

Fig. 3.1. Poles and zeros of a flexible beam with collocated sensor and actuator.

Lemma 3.1

Suppose the position sensor is collocated with the actuator at $x_j = 0$. Then, the transfer function (3.7) has the form

$$P = k \frac{\sum_{i=1}^{n}(s^2 + \omega_i^2)}{s^2 \sum_{i=1}^{n}(s^2 + p_i^2)}$$

such that k is real,

$$\omega_{i+1} > \omega_i > 0,$$

$$p_{i+1} > p_i > 0,$$

and

$$\omega_{i+1} > p_i > \omega_i ,$$

for all i.

The proof is omitted here, and can be established by using the results in [20].

Now, suppose that the sensor location x_j varies along the beam. It can be seen from equation (3.7), that the poles of the system remain invariant with respect to x_j. However, the loci of the plant zeros is affected by changes in x_j. The zeros have an interesting loci which is described by the following theorem.

Theorem 3.1

Suppose the location x_j of the position sensor varies from 0 (collocated with the actuator) to L (end-tip). Then,

1. The zero loci is a continuous function of x_j.
2. The initial portion of each branch of the loci, in the upper half of the

complex plane, lies on a section of the imaginary axis. This section starts from $j\omega_i$ i = 1, ..., n and extends in the upward direction (Fig. 3.5).

3. If $\sum_{i=1}^{n} \Phi_i \phi_i = 1$, the plant P has a zero at infinity; and if $\sum_{i=1}^{n} \Phi_i \phi_i > 1$, at least one zero becomes nonminimum-phase.

Proof

1. Consider n flexibility modes. The numerator $b_n(s)$ of the transfer function (3.7) is a polynomial of degree n and is given by

$$\rho L\, b_n(s) = a_n(s) = \prod_{i=1}^{n}(s^2 + \omega_i^2) - \sum_{i=1}^{n} s^2 \Phi_i \phi_i(x_j) \prod_{\substack{j=1 \\ j \neq i}}^{n}(s^2 + \omega_j^2). \tag{3.8}$$

Let $K_i = \Phi_i \phi_i(x_j)$ i = 1, ..., n. It is known that the roots of a polynomial are continuous functions of the coefficients. It is also clear from (2.17) that the parameter K_i is a continuous function of x_j. Therefore, the zero loci (roots of $b_n(s)$) is a continuous function of x_j.

2. Part 2 of the theorem is proved by induction, using root locus arguments for positive feedback systems.

We first show that K_i i = 1, ..., n is positive for x in some interval $(0, x_d)$. For this, note that

$$\Phi_i = \frac{2(\cosh(k_iL) + \cos(k_iL))}{k_iL\,(\sinh(k_iL) + \sin(k_iL))}$$

is positive for all i. Moreover, there exists x_d, $0 \le x_d \le L$, so that all mode shapes $\phi_i(x)$ are positive for x in $(0, x_d)$. Indeed, it can be seen from (2.17) that the

asymptotic expansion of $\phi_i(x)$ near zero is $k_i^2 x^2$ for all i. Hence, $K_i = \Phi_i \phi_i$ is positive in $(0, x_d)$ for all i.

Let $\lambda = s^2$, and consider n = 1. The polynomial $a_1(\lambda)$ can be written as

$$a_1(\lambda) = (\lambda + \omega_1^2) - \lambda K_1. \tag{3.9}$$

It can be verified that $0 \le K_1 \le 1.54$ for $0 \le x \le L$. Equation (3.9) can be viewed as a positive feedback closed-loop system, with K_1 being the positive feedback gain, the root of $P_1(\lambda) = \lambda + \omega_1^2$ being the open-loop pole, and the root of $Q_1(\lambda) = \lambda$ being the open-loop zero. Therefore, the root loci of $a_1(\lambda)$ is as shown in Fig. 3.2, when the gain K_1 is increased from zero to infinity.

In the case n = 1, it is obvious that the section $[j\omega_1, \infty]$ of the imaginary axis is part of the zero loci as x varies from 0 to L (Fig. 3.3).

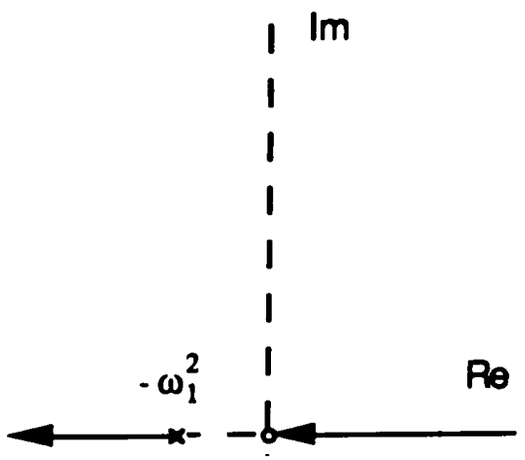

Fig. 3.2 Root loci of $a_1(\lambda)$, as a function of $K_1 = \Phi_1 \phi_1$.

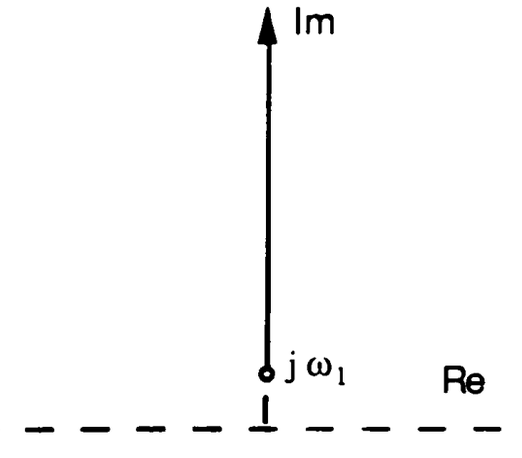

Fig. 3.3 Plant zero loci, as a function of x_j, for n = 1.

Consider the case n = 2. The plant numerator $a_2(\lambda)$ can be put in the form

$$a_2(\lambda) = (\lambda + \omega_2^2)\, a_1(\lambda) - K_2 \lambda\, (\lambda + \omega_1^2). \tag{3.10}$$

Let p_1, p_2 be the roots of $a_2(\lambda)$ and p_1' be the root of $a_1(\lambda)$ so that

$$-\omega_2^2 < p_1' < -\omega_1^2.$$

Again, equation (3.10) can be considered as a positive feedback system. The loci of the roots of $a_2(\lambda)$, as the positive gain K_2 is varied from zero, has the form of Fig. 3.4. When $x = 0$ ($K_1 = K_2 = 0$), the roots of $a_2(\lambda)$ are at $-\omega_1^2$ and $-\omega_2^2$. As seen in part 1, the zero loci is a continuous function of x. Furthermore, $K_i \sim \Phi_i k_i^2 x^2$ is positive in the neighborhood of zero. Thus, there exists a sufficiently small nonzero δ such that, for x in (o, δ), $-\omega_2^2 < p_1' < -\omega_1^2$ and the roots of $a_2(\lambda)$ satisfy

$$\begin{aligned} -\omega_2^2 < p_1 < -\omega_1^2 \\ p_2 < -\omega_2^2. \end{aligned} \tag{3.11}$$

Equivalently, the initial part of each branch of the loci is a section of the imaginary axis which starts from $j\omega_i$, $i = 1, 2$ and extends in the upward direction of the imaginary axis (Fig. 3.5).

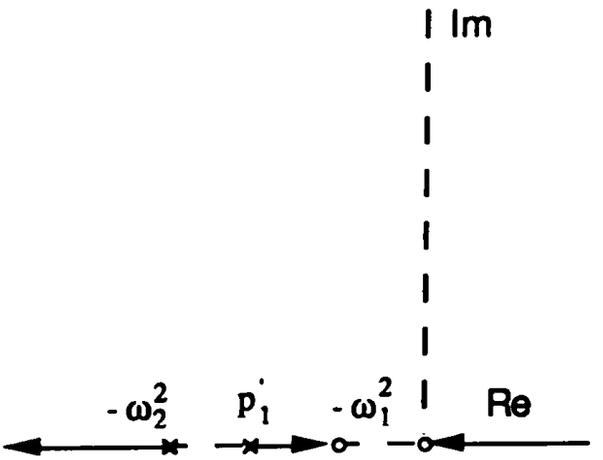

Fig. 3.4. Root loci of $a_2(\lambda)$ as a function of K_2.

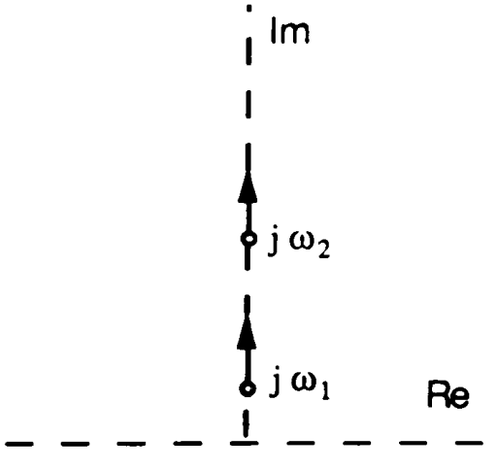

Fig. 3.5. Plant zero loci, as a function of x_j, for n = 2.

Consider n flexibility modes and define $p_1, \ldots, p_n$ as the real roots of $a_n(\lambda)$. Assume there exists a sufficiently small δ_1 such that for x in $(0, \delta_1)$ we have

$$\begin{aligned} -\omega_{i+1}^2 < p_i < -\omega_i^2, \quad i = 1, \ldots, n-1 \\ p_n < -\omega_n^2 \end{aligned} \tag{3.12}$$

For n+1 elastic modes, $a_{n+1}(\lambda)$ can be expressed as

$$a_{n+1}(\lambda) = (\lambda + \omega_{n+1}^2)\, a_n(\lambda) - K_{n+1}\, \lambda \prod_{i=1}^{n} (\lambda + \omega_i^2). \tag{3.13}$$

Under assumptions (3.12), the root loci of $a_{n+1}(\lambda)$, as a function of K_{n+1}, is as shown in Fig. 3.6. Note that if $p_n < -\omega_{n+1}^2$, the loci still have the same pattern. Fig. 3.6 indicates that at x = 0 the roots of $a_{n+1}(\lambda)$ are at $-\omega_i^2$ i =1, ..., n+1. Again, the zero loci is a continuous function of x, and $K_i \sim \Phi_i k_i^2 x^2$ is positive near zero. It follows that there exists a sufficiently small nonzero $\delta_2 \le \delta_1$ such that, the ith root of $a_{n+1}(\lambda)$ is located to the left of $-\omega_i^2$ and satisfies assumptions (3.12) for x in $(0, \delta_2)$ and i = 1, ..., n+1. That is, by induction, assumptions (3.12) are true. Consequently, the initial portion of each branch of the loci lies on a section of the imaginary axis. This section starts from $j\omega_i$ i = 1, ..., n and extends in the positive direction of the imaginary axis.

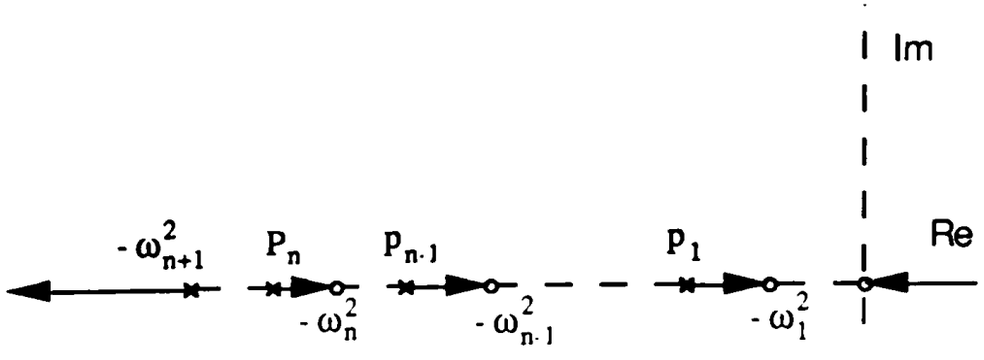

Fig. 3.6. Root loci of $a_{n+1}(\lambda)$, function of $K_n = \Phi_{n+1}\, \phi_{n+1}$.

3. In part 3 of the proof, we want to establish first that $a_n(\lambda)$ has a zero at infinity for some values of the gains K_i. The polynomial $a_n(\lambda)$ can be written as

$$a_n(\lambda) = \prod_{i=1}^{n} (\lambda + \omega_i^2) - \sum_{i=1}^{n} K_i \lambda \prod_{\substack{j=1 \\ j \neq i}}^{n} (\lambda + \omega_j^2). \tag{3.14}$$

Let $\alpha = 1/\lambda$. Subsitution into (3.14) yields

$$a_n(\alpha) = \alpha^{-n} [\prod_{i=1}^{n} (1 + \alpha\, \omega_i^2) - \sum_{i=1}^{n} K_i \prod_{\substack{j=1 \\ j \neq i}}^{n} (1 + \alpha\, \omega_j^2)] = \alpha^{-n} \Psi(\alpha). \tag{3.15}$$

By definition, $a_n(\lambda)$ has a zero at infinity if and only if the polynomial $\Psi(\alpha)$ has a root at $\alpha = 0$. It can be seen from (3.14) that if $\sum_{i=1}^{n} K_i = 1$, then $\alpha = 0$ is a root of $\Psi(\alpha)$. From this we conclude that when $\sum_{i=1}^{n} K_i = 1$, the plant has a zero at infinity.

Next, we show that at least one zero becomes nonminimum-phase when $\sum_{i=1}^{n} K_i > 1$. Notice that the leading coefficient of $a_n(\lambda)$ is $1 - \sum_{i=1}^{n} K_i$, and that the constant term is $\prod_{i=1}^{n} \omega_i^2$. It is then clear that if $\sum_{i=1}^{n} K_i > 1$, a sign change occurs in the coefficients of $a_n(\lambda)$; ie. at least one root of $a_n(\lambda)$ is in the open RHP. In other words, at least one plant zero is nonminimum-phase. This concludes the proof.

We have verified numerically, that the value $\sum_{i=1}^{n} K_i > 1$ is attainable in the interval $0 \leq x \leq L$, say for $n \leq 50$. That is, nonminimum-phase zeros will appear as x_j varies from 0 to L. We also noticed that the larger the number n of elastic modes, the smaller the value of x for which nonminimum-phase zeros appear. This may be

explained by the fact that, in the neighborhood of $x = 0$, $\sum_{i=1}^{n} K_i \sim \sum_{i=1}^{n} k_i^2 \Phi_i x^2$ increases with n.

Example 3.1

Consider a 3 ft. long aluminum beam as depicted in Fig. 2.1. The finite dynamic model includes the first five flexibility modes (n = 5). Fig. 3.7 shows the zero loci for a collocated position sensor. In Fig. 3.8, For $x_j = 0.3$ft., the last zero is still on the imaginary axis, but has moved across the highest pole. When $x_j = 0.55$ft. (Fig. 3.9), one nonminimum-phase zero appears on the real axis. Fig. 3.10 shows the zero pattern for a sensor at the tip. In this particular case, all zeros have left the imaginary axis, and five of them are nonminimum-phase.

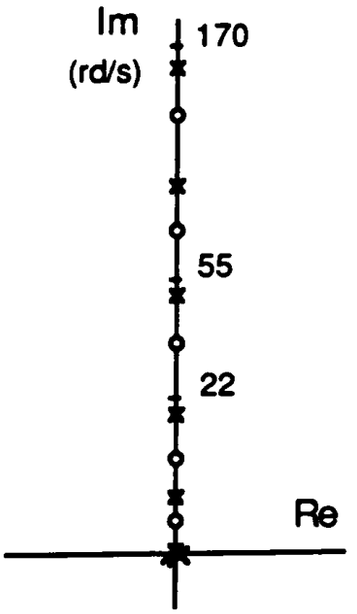

Fig. 3.7. Pole-zero pattern for $x_j = 0$ ft. (collocated).

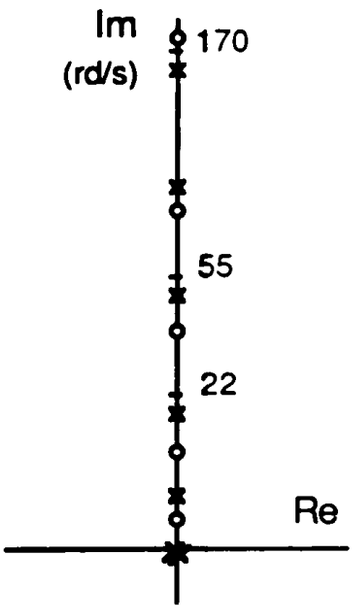

Fig. 3.8. Pole-zero pattern for $x_j = 0.3$ ft.

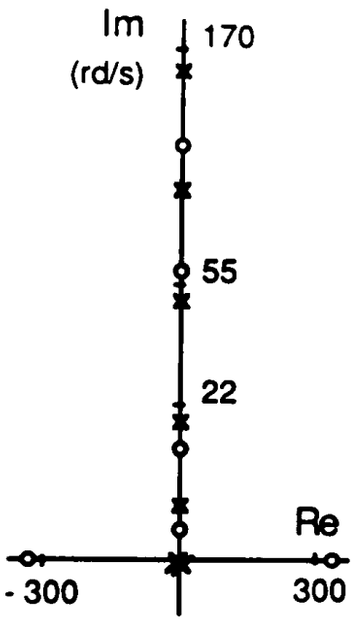

Fig. 3.9. Pole-zero pattern for $x_j = 0.55$ ft.

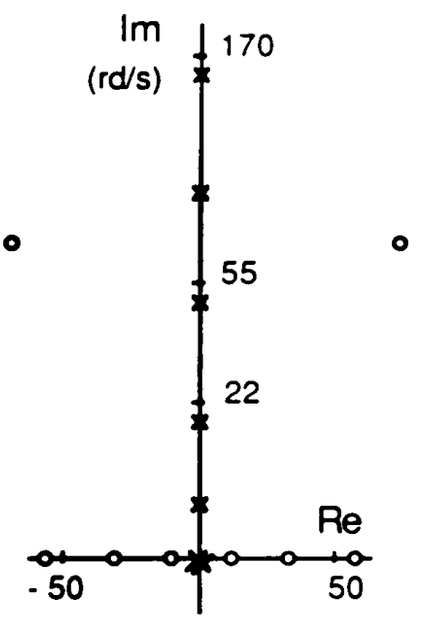

Fig. 3.10. Pole-zero pattern for $x_j = 3$ ft. (at tip).

3.1.2 Conclusions

In the collocated case, the interlacing property of the poles and zeros is well known, and has often been used by designers for rocket and spacecraft control. Noncollocated configurations have been studied by Canon and Shmitz [21]. In their experiment, a position sensor is placed at the tip of a flexible beam. The ensuing actuator tip-sensor transfer function is nonminimum-phase, and has the shape of Fig. 3.10. That is our results are consistent with the zero patterns identified experimentally by other authors.

Because of physical constraints or some particular performance needs, exact collocation may not be possible. This implies that the regular alternation of poles and zeros may not be obtained, and the control synthesis becomes more difficult. For instance, consider the case of small displacements of the sensor from the collocated location. In general, the interlacing pattern for lower-order modes can be maintained. However, the higher-order zeros can cross the invariant poles. It results in a set of

regularly alternating poles and zeros, followed by a set of poles and zeros with a reversed interlacing as shown in Fig. 3.8. Notice that at the boundary, there are two consecutive poles. For such plants, a suitable compensation technique is not as apparent as for a collocated arrangement; this situation is dealt with in section 3.3. Now, if the sensor is placed far enough from the actuator, some nonminimum-phase zeros appear, which imposes severe limitations on control synthesis.

3.2 Frequency-minimax control design

As shown in the preceding section, a noncollocated selection of the actuator and the sensor can give rise to complicated control design problems. Some authors have proposed solutions to this problem by applying optimal LQ and LQG methodologies [21]. In this section we present a robust design methodology applicable to this problem. The technique uses Kwakernaak's frequency-domain optimization approach. We also emphasize the choice of the weightings in the cost function, and give a search procedure which always yields the optimal stable solution.

A robust controller is a controller which can maintain some properties, such as stability, under uncertainties in the actual plant parameters. For SISO systems, commonly used measures of robustness are the Bode/Nyquist gain and phase margins. These margins are often incorporated into the specifications of a control system design. Horowitz [22], for example, combines these frequency response measures with root-locus methodologies to meet explicit specifications on disturbances, parameter variations, etc. It has been established that robustness may be simultaneously expressed as a function of the sensitivity and its complement. Zames [23] has formulated the sensitivity reduction problem as an optimization problem; and has obtained stable feedback schemes. Kwakernaak [24] has extented Zames' work and characterized robustness as a minimax problem of both the

sensitivity function and its complement. A nice feature of Kwakernaak's approach is its ability to handle poles and zeros on the jω-axis (singularities), ie. plants of the form (3.3).

3.2.1 Kwakernaak's minimax approach

In this section we briefly present the procedural aspects of Kwakernaak's methodology. For more details, the reader is referred to [24, 25].

Consider a SISO plant $P = \Psi/\Phi$ with $\deg \Phi = n$, $\deg \Psi = m$, $m \leq n$. Let $G = \rho/\sigma$ be a proper stabilizing compensator. The sensitivity function S and its complement T can be written as

$$S = (1 + GP)^{-1} = \Phi\sigma/\chi_{cl}, \quad T = 1 - S = \Psi\rho/\chi_{cl} \tag{3.16}$$

where, χ_{cl} is the closed-loop characteristic polynomial given by $\chi_{cl} = \Phi\sigma + \Psi\rho$.

Suppose, the real perturbed plant is $P = \Psi'/\Phi'$. The resulting closed-loop characteristic polynomial is $\chi'_{cl} = \Phi'\sigma + \Psi'\rho$. Therefore,

$$\frac{\chi'_{cl}}{\chi_{cl}} - 1 = \left(\frac{\Phi'}{\Phi} - 1\right) S + \left(\frac{\Psi'}{\Psi} - 1\right) T \tag{3.17}$$

Equation (3.17) indicates, by the principle of argument, that the perturbed closed-loop system remains stable if and only if the RHS does not encircle the point -1 + j0. Hence, a sufficient condition for stability is that the magnitude of the RHS be less than one. This analysis leads to a robust criterion involving a weighted combination of the sensitivity S and its complement T of the form

$$Z(s) = |V(j\omega)\, S(j\omega)|^2 + |W(j\omega)\, T(j\omega)|^2 \tag{3.18}$$

where, V and W are suitable weighting functions. Robustness optimization is then defined as the problem of minimizing

$$\sup_{\omega} (|V(j\omega)\, S(j\omega)|^2 + |W(j\omega)\, T(j\omega)|^2). \tag{3.19}$$

Kwakernaak has solved this minimax problem by reducing it to solving a nonlinear system of equations. More precisely, it can be shown that if a stabilizing controller exists, then it is unique and it satisfies

$$Z(s) = \lambda^2 \tag{3.20}$$

where, λ is a real and λ^2 is the minimum value of the cost. Let $\Phi = \Phi_- \Phi_0 \Phi_+$ and $\Psi = \Psi_- \Psi_0 \Psi_+$, where $\deg(\Phi_-) = n_-$, $\deg(\Phi_0) = n_0$, $\deg(\Phi_+) = n_+$, $\deg(\Psi_-) = m_-$, $\deg(\Psi_0) = m_0$, $\deg(\Psi_+) = m_+$; such that Φ_- and Ψ_- have their roots in the open LHP, Φ_0 and Ψ_0 have their roots on the imaginary axis, Φ_+ and Ψ_+ have their roots in the open RHP. Let V and W be

$$V(s) = \frac{\alpha_1(s)}{\beta_1(s)}, \quad W(s) = \frac{\alpha_2(s)}{\beta_2(s)} \tag{3.21}$$

such that $\beta_1(s) = \beta_1'(s)\, \Phi_0$ with $\deg(\beta_1) = b_1$, $\deg(\alpha_1) = a_1$; $\beta_2(s) = \beta_2'(s)\, \Psi_0$ with $\deg(\beta_2) = b_2$, $\deg(\alpha_2) = a_2$. If the compensator G is chosen as

$$G = \frac{\rho}{\sigma} = \frac{\Phi_- \beta_2' \xi}{\Psi_- \beta_1' \theta} \tag{3.22}$$

then, (3.20) can be written as a nonlinear system of equations of the form

$$\alpha_1 \alpha_1^* \Phi_+ \Phi_+^* \theta\, \theta^* + \alpha_2 \alpha_2^* \Psi_+ \Psi_+^* \xi\, \xi^* = \lambda^2 \chi\, \chi^* \tag{3.23}$$

where, $\chi = \Phi_+ \beta_1 \theta + \Psi_+ \beta_2 \xi$, and the characteristic polynomial is $\chi_{cl} = \Phi_- \Psi_- \chi$.

The optimization problem has a solution under the following assumptions

a) $a_1 \le b_1$, $a_2 = b_2 + e$, $e = n - m$.

b) α_1 and α_2 have all their roots in the closed LHP; β_1 and β_2 have all their roots in the closed-loop LHP and have no common roots; α_1 and β_1 have no common roots; α_2 and β_2 have no common roots.

c) The polynomial $\gamma = \alpha_1 \alpha_1^* \beta_2 \beta_2^* + \alpha_2 \alpha_2^* \beta_1 \beta_1^*$ has no roots on the imaginary axis.

d) The roots of β_1 and β_2 are also roots of, respectively, $\Phi_0 \Phi_-$ and $\Psi_0 \Psi_-$.

Let a polynomial η be

$$\eta = \alpha_1 \alpha_1^* \alpha_2 \alpha_2^* .$$

A polynomial π_λ is defined, for those λ for which it exists, as

$$\pi_\lambda \pi_\lambda^* = \gamma - \frac{1}{\lambda^2} \eta \tag{3.24}$$

π_λ is well -defined for $|\lambda| > \lambda_0 \geq 0$, where λ_0 is the first value of λ for which (3.24) loses degree or assumes a root on the imaginary axis. Define, $x = n_+ + m_+ + b_1 + b_2 + e$, $t = m_+ + b_2 + e$, $z = n_+ + b_1$. The existence of the solution of (3.23) is given by the following theorem.

Theorem 3.2

Assume that assumptions a) through d) hold, and suppose χ_{λ_0} or $\chi_{-\lambda_0}$ has at least one root in the RHP. Then, there exists a λ with $|\lambda| > \lambda_0 \geq 0$ such that $\deg(\chi_\lambda) = x - 1$, $\deg(\theta_\lambda) = t - 1$, $\deg(\xi_\lambda) = z - 1$; and χ_λ has all its roots in the open LHP. Furthermore, the controller $(\theta_\lambda, \xi_\lambda)$ uniquely minimizes (3.19) and the minimal value is λ^2.

The proof of this theorem is given in [24].

Remarks

1. The roots of the polynomial γ are the closed-loop poles (of χ_λ) for $|\lambda| = \infty$.

2. If χ_{λ_0} is unstable, the optimal reduced-order compensator is of order n - 1.

3. The nonlinear system (3.4) is well-determined with unknowns λ and the controller parameters (θ, ξ).

3.2.2 Robust control of flexible structures

Because of the very high-order of the FEM representation of a flexible structure, a practical compensator has to be based on a reduced-order design model (ROM). Typically, the ROM consists of the rigid-body modes and a number of low-frequency elastic modes. Suppose that the dynamics of the flexible structure in consideration has one rigid-body mode, and that the truncated design model includes n_1 flexibility modes, $n_1 \leq k$ so that the ROM P_n has the form

$$P_n = \frac{\Psi}{\Phi} = \frac{1}{s^2} + \sum_{i=1}^{n_1} \frac{r_i a_i}{s^2 + \omega_i^2} = \frac{b_1 s^m + \ldots + b_{n-1} s + b_n}{s^n + a_1 s^{n-1} + \ldots + a_n} \tag{3.25}$$

with $m \leq n$.

Now, we apply Kwakernaak's minimax method to design a robust compensation for the plant P_n. In the case where the zeros of P_n also lie on the imaginary axis, a suitable choice of the weightings V and W is found to be

$$V(s) = \frac{1 + \tau_1 s}{\tau_1^2 \Phi}, \qquad W(s) = \frac{\tau_2 s^{m+2}}{\Psi} \tag{3.26}$$

where τ_1, τ_2 are positive constant design parameters. It can be easily verified that these weightings satisfy assumptions a) through d) of theorem 3.2.

It was mentioned previously that the roots of the polynomial γ are closed-loop poles for $|\lambda| = \infty$. For a stable closed-loop design, plant poles and zeros on the imaginary axis are included in, respectively, β_1 and β_2. When these open-loop poles and zeros are closely clustered, the roots of the polynomial γ can be very near the imaginary axis. This can complicate the search for the stable solution as $|\lambda|$ is decreased form infinity (roots can cross the imaginary axis into the RHP). The above choice of V anfd W gave the best stability margins at $|\lambda| = \infty$.

The optimal value λ_0, for which (3.24) loses degree, is found to be

$$\lambda_0 = \frac{\tau_1^2 \tau_2^4}{\tau_1^2 + \tau_1^4 \tau_2^4} \tag{3.27}$$

With V and W as given by (3.26), the optimal controller may be obtained by solving the nonlinear system (3.23) of degree 2n. In most situations the optimal solution χ_{λ_0} turns out to be unstable. Thus, one has to solve for the reduced-order solution χ_λ for $|\lambda| \geq \lambda_0$.

At this point we make some important remarks on the numerical aspects of solving the nonlinear system (3.23). Obviously, solving a nonlinear system of equations is among the hardest numerical problems one may encounter. Most of the recent codes tackle the problem as an unconstrained optimization (trust region, linesearch [26]). These global methods converge only toward a local zero or minima, and no fool-proof algorithm is available. Another difficulty in solving (3.23) is that we are seeking the unique reduced-order solution among all possible solutions (3.23) might have. This amounts to finding a 'good starting guess'. A linear least-square estimation procedure of the initial guess is proposed in [24], but in most cases the result is a poor estimate. Because, first the overdetermined linear system depends on the unknown λ itself. Secondly, the degree of overdetermination is too high. For

example, consider the flexible beam control problem of e.g. 3.3, where the ROM design plant is of order 4. To solve the nonlinear system of order 8, we used the modified linesearch algorithm [26]. The estimation procedure of the starting point consists of solving a system of 16 linear equations in seven unknowns; and the estimate fails to converge toward the desired stable solution. The convergence is to χ_{λ_0} which is unstable. Other starting points were tried unsuccessfully. In the subsequent section we present a method that would always converges to the optimal stable design.

3.2.3 Search procedure for the optimal stabilizing controller

To avoid the problem of searching for the stable solution among all possible solutions of (3.23), we take the following approach. We know that when assumptions a) through d) are satisfied, there exists a unique stabilizing compensator of order (n-1) which minimizes (3.19). Moreover, this compensator is such that Z(s) = λ^2. Suppose one can parametrize all stabilizing controllers of order (n-1). If the parametrization is substituded in Z(s) = λ^2, the resulting nonlinear system has a unique stable solution which is the optimal stabilizing controller.

Precisely, let G = σ/ρ be an (n-1) parametrization of all the stabilizing controllers. Then, Z(s) = λ^2 can be written as

$$k_2 \Phi_- \Phi_-^* \Phi_+ \Phi_+^* \alpha_1 \alpha_1^* \sigma \sigma^* + k_1 \Psi_- \Psi_-^* \Psi_+ \Psi_+^* \alpha_2 \alpha_2^* \rho \rho^* = \lambda^2 k \chi_{cl} \chi_{cl}^* \tag{3.28}$$

where χ_{cl} is the corresponding closed-loop polynomial, $k_1 = \beta_1' \beta_1'^*$, $k_2 = \beta_2' \beta_2'^*$, and $k = k_1 k_2$.

example, consider the flexible beam control problem of e.g. 3.3, where the ROM design plant is of order 4. To solve the nonlinear system of order 8, we used the modified linesearch algorithm [26]. The estimation procedure of the starting point consists of solving a system of 16 linear equations in seven unknowns; and the estimate fails to converge toward the desired stable solution. The convergence is to χ_{λ_0} which is unstable. Other starting points were tried unsuccessfully. In the subsequent section we present a method that would always converges to the optimal stable design.

3.2.3 Search procedure for the optimal stabilizing controller

To avoid the problem of searching for the stable solution among all possible solutions of (3.23), we take the following approach. We know that when assumptions a) through d) are satisfied, there exists a unique stabilizing compensator of order (n-1) which minimizes (3.19). Moreover, this compensator is such that Z(s) = λ^2. Suppose one can parametrize all stabilizing controllers of order (n-1). If the parametrization is substituded in Z(s) = λ^2, the resulting nonlinear system has a unique stable solution which is the optimal stabilizing controller.

Precisely, let G = σ/ρ be an (n-1) parametrization of all the stabilizing controllers. Then, Z(s) = λ^2 can be written as

$$k_2 \Phi_- \Phi_-^* \Phi_+ \Phi_+^* \alpha_1 \alpha_1^* \sigma \sigma^* + k_1 \Psi_- \Psi_-^* \Psi_+ \Psi_+^* \alpha_2 \alpha_2^* \rho \rho^* = \lambda^2 k \chi_{cl} \chi_{cl}^* \tag{3.28}$$

where χ_{cl} is the corresponding closed-loop polynomial, $k_1 = \beta_1' \beta_1'^*$, $k_2 = \beta_2' \beta_2'^*$, and $k = k_1 k_2$.

Now, the nonlinear system (3.28) has a unique stable solution. The parametrization can be accomplished the following fashion. Consider the diophontine equation

$$\chi_{cl} = \Phi\,\sigma + \Psi\,\rho. \tag{3.29}$$

Let χ_{cl} belong to the set of all stable polynomials of degree 2n - 1, ie. χ_{cl} can be expressed as

$$\chi_{cl} = \prod_{i=1}^{2n-1}(s + p_i) = s^{2n-1} + d_1\,s^{2n-2} + \ldots + d_{2n-1} \tag{3.30}$$

where, p_i, i = 1, ..., 2n-1 are in the open LHP. This normalized form of χ_{cl} ensures a well-determined nonlinear system of equations (3.28). Let the parametrized compensator G of order (n-1) be

$$G = \frac{\rho}{\sigma} = \frac{m_1\,s^{n-1} + m_2\,s^{n-2} + \ldots + m_n}{s^{n-1} + n_1\,s^{n-2} + \ldots + n_{n-1}}. \tag{3.31}$$

Then, equation (3.29) can be written as

$$S(\Phi, \Psi)\,G = W \tag{3.32}$$

where,

$$S = \begin{bmatrix} 1 & 0 & \cdots & 0 & b_1 & 0 & \cdots & 0 \\ a_1 & 1 & & & b_2 & b_1 & & 0 \\ \vdots & \vdots & & \vdots & \vdots & \vdots & & \vdots \\ a_{n-1} & a_{n-2} & & a_1 & b_n & b_{n-1} & & b_1 \\ a_n & a_{n-1} & & a_2 & 0 & b_n & & b_2 \\ 0 & a_n & & & 0 & & & \vdots \\ \vdots & \vdots & & \vdots & \vdots & \vdots & & \\ 0 & 0 & \cdots & a_n & 0 & 0 & \cdots & b_n \end{bmatrix} \tag{3.33}$$

is a (2n-1) square matrix, and

$$G = (n_1 \ldots n_{n-1} \; m_1 \ldots m_n)^t ,$$

$$W = (d_1 - a_1 \ldots d_n - a_n \; d_{n+1} \ldots d_{2n-1})^t$$

therefore, the compensator G is

$$G = S^{-1}(\Phi, \Psi)\, W. \tag{3.34}$$

Equation (3.34) is precisely the parametrization of all the reduced-order (n-1) controllers. The free parameters $d_1, \ldots, d_{2n-1}$ are such that χ_{cl} belongs to the set of all stable polynomials.

Lemma 3.2

The matrix S is nonsingular if and only if the pair (Φ, Ψ) is coprime.

Proof

The proof is established by contradiction. Suppose the matrix $S(\Phi, \Psi)$ is singular. Then, there exists a nonzero vector $V = [v_1, \ldots, v_{2n-1}]$ such that

$$S(\Phi, \Psi)\, V = 0. \tag{3.35}$$

Let $p(s) = s^{n-1} + v_1 s^{n-2} + \ldots + v_{n-1}$ and $q(s) = v_n s^{n-1} + v_{n+1} s^{n-2} + \ldots + v_{2n-1}$. Equation (3.35) can be rewritten as

$$\Phi(s)\, p(s) + \Psi(s)\, q(s) = 0 \tag{3.36}$$

and if p(s) and q(s) are nonzero, we have

$$\frac{\Phi}{\Psi} = -\frac{q}{p} \tag{3.37}$$

But (3.37) is not possible if (Φ, Ψ) is coprime. This establishes the proof.

Remarks

1. The new variables of the nonlinear system (3.28) are the free parameters $d_1, \ldots, d_{2n-1}$ and λ. After the solution is obtained, the optimal compensator is derived from (3.34).

2. In examples 3.3 and 3.4, the closed-loop polynomial χ_{cl} is of order 7. One can parametrize the set of all stable polynomials of degree 7 as $\chi_{cl} = (s + r^2) \prod_{i=1}^{3} [(s + g_i^2)^2 + h_i^2]$; where r, g_i, h_i are arbitrary numbers. This representation is one of the four possible closed-loop configurations.

3.2.4 Design examples

Example 3.2: Double integrator

Here, we consider the same example as in [24] to show the effectiveness of the proposed search algorithm. Let the plant $P(s) = 1/s^2$. The weightings V and W are chosen as in [24], ie.

$$V V^* = \frac{1 + (\tau_1 s)^4}{(\tau_1 s)^4}, \text{ and } W = (\tau_2 s)^2.$$

To solve the minimax problem we used both the direct method (3.23) and the parametrization procedure. In either case, the resulting nonlinear system is of order 4. For $\tau_1 = \tau_2 = 1$, table 3.1 shows the numerical solutions obtained with two different starting points, a far away point and a closer one. In both cases, the direct method converges to an unstable zero, whereas the parametrization algorithm converges to the optimal stable solution.

Example 3.3: Flexible beam control

In this example we consider the control of a flexible aluminum beam, as depicted in Fig. 2.1, with a length L = 3ft. For a collocated sensor and actuator, the transfer function for the first 5 elastic modes is given by Fig. 3.11. A design ROM P_4 is taken to consist of the rigid-body mode and the first flexibility mode such that

$$P_4 = \frac{0.0121(s^2 + 6.67)}{s^2(s^2 + 17.24)} .$$

Then, the minimax approach was applied (based on the ROM) to obtain an optimal robust compensator of order 3. We have already mentionned that with the direct method we could not find a suitable starting point that leads to the stable design. With the parametrization scheme, the procedure has converged to the stabilizing solution with a satisfactory precision. Table 3.2 shows the minimax compensators obtained with two sets of design parameters (τ_1, τ_2).

Given these optimal solutions, we simulated the closed-loop compensated system. In the simulation, the 12th-order plant of Fig. 3.11 was used as an evaluation model to take into account the effect of the the unmodelled higher-frequency dynamics (spillovers). The closed-loop poles of the resulting nominal

system are given by table 3.2. Figures 3.12 - 3.14 show the response to a step unit and the frequency Bode plots for ($\tau_1 = 1.6$, $\tau_2 = 0.04$).

To test the robustness of the controller, we simulated the closed-loop system with a 30% decrease in the five frequency modes of the evaluation model. Table 3.3 gives the closed-loop poles of the system, under the simulated uncertainties, for the minimax design and for a standard state-feedback observer design (based on the given ROM P_4). Note that only the minimax design remains stable.

Example 3.4: Noncollocated control

As we mentioned earlier, when the sensor is not collocated with the actuator, the transfer function will not have the regular interlacing of poles and zeros (Fig. 3.1). In this example, we treat such noncollocated configuration, and consider the 12th-order transfer function of Fig. 3.15. Notice the reversed alternation of poles and zeros on the imaginary axis, and the presence of a nonminimum-phase zero. A 3rd-order minimax controller is obtained based on a ROM P_4 which consists of the rigid-body and the first flexibility mode, ie.

$$P_4 = \frac{0.16\,(s^2 + 88.66)}{s^2\,(s^2 + 69.38)}\,.$$

Table 3.4 shows solutions for two sets of (τ_1, τ_2). It also gives the closed-loop poles of the nominal compensated system, in which the evaluation model is the 12th-order plant of Fig. 3.15.

We also verified the robustness of the design by lowering the frequency modes by 30% in the evaluation model. Table 3.5 gives the results for the minimax compensator ($\tau_1 = 0.5$, $\tau_2 = 0.07$), and for a state-feedback observer design. Again, note the better robustness of the frequency optimization design.

3.2.5 Conclusions

In this section we have presented a minimax compensation technique for the robust control of flexible structures. We have also developed a search procedure which always converges to the optimal stabilizing solution. Then, the minimax approach was compared to state-space optimal methods. It is our experience that controllers obtained with the minimax design have better robustness properties.

3.3 Generalized lead-lag compensation technique

We have shown in the beginning of this section, for a class of flexible beams, that as the sensor is displaced away from the actuator, the zeros move upward along the jω-axis. Starting with the highest mode, the zeros will cross the poles while the poles remain invariant. At some point, the zeros break into the complex plane in a nonminimum-phase fashion.

Before the zeros break into complex patterns, ie. for small positional gaps between the actuator and the sensor, the system model has the form of Fig. 3.16.

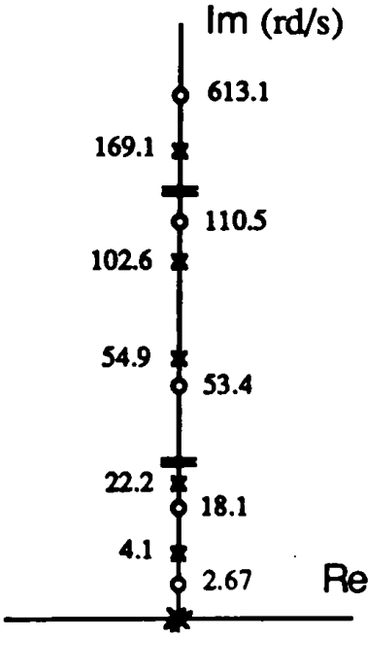

Fig. 3.16 Plant pole-zero locus of the beam with a sensor located at $x_j = 0.5$ ft.

Table 3.1 Comparaison of the minimax direct method and the parametrization scheme for a plant $G(s) = 1/s^2$.

$\tau_1=1$ $\tau_2=1$	Starting point	Numerical solution			
Direct method		θ_2	ξ_1	ξ_2	λ
	.7 .4 .7 3	-.68	-.21	.67	1.02
	-20 20 10 20	-.68	-.21	.67	1.02
parametrization approach		n_1	m_1	m_2	λ
	.7 .4 .7 3	2.34	2.18	.98	2.34
	-20 20 10 20	2.34	2.18	.98	2.34

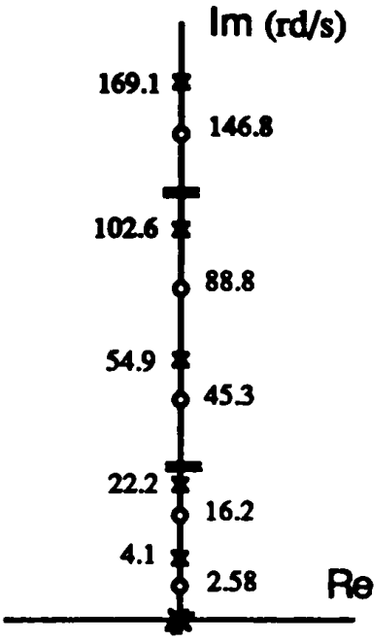

Fig. 3.11 Plant of the flexible beam with a collocated sensor and actuator.

Table 3.2 Minimax design for the flexible beam with $x_j = 0$. Nominal closed-loop system.

$\tau_1 = 1.6$ $\tau_2 = .04$		$\tau_1 = 0.5$ $\tau_2 = 0.1$	
minimax Compensator	Closed-loop poles	minimax Compensator	Closed-loop poles
$\lambda = .025$ $n_1 = 16.16$ $n_2 = 30.14$ $n_3 = 147.54$ $m_1 = 6319.1$ $m_2 = 13431$ $m_3 = 69445$ $m_4 = 28834$	-.62 -.63 ± j 2.89 - 3.73 ± j 2.1 - 2.54 ± j 3.71 -. 66 ± j 23.24 -.14 ± j 55.44 -.043 ± j 102.9 -.027 ± j 169.4	$\lambda = .025$ $n_1 = 9.84$ $n_2 = 8.88$ $n_3 = 62.25$ $m_1 = 2445.6$ $m_2 = -1594.9$ $m_3 = 18323$ $m_4 = 12616$	- 1.86 - 2.33 ± j 1.45 -.29 ± j 2.47 - 1.09 ± j 3.12 -.22 ± j 22.6 -.04 ± j 55.1 -.012 ± j 102.7 -.008 ± j 169.2

Table 3.3 Effect of model-parameter variations upon stability of closed-loop system.

Closed-loop poles of compensated system under 30% decrease in all frequency modes of the evaluation model	
Minimax design ($\tau_1 = 1.6$, $\tau_1 = 0.04$)	State-space design
-.61 -.6 ± j 1.75 -.97 ± j 3.15 - 4.64 ± j 4.23 - 1.1 ± j 16.8 -.27 ± j 39.2 -.09 ± j 72.3 -.055 ± j 118.8	-.508 - 9.66 -.36 ± j .55 + .36 ± j 1.76 - 3.84 ± j 4.26 + .08 ± j 15.88 + .06 ± j 38.47 + .02 ± j 71.8 + .01 ± j 118.4

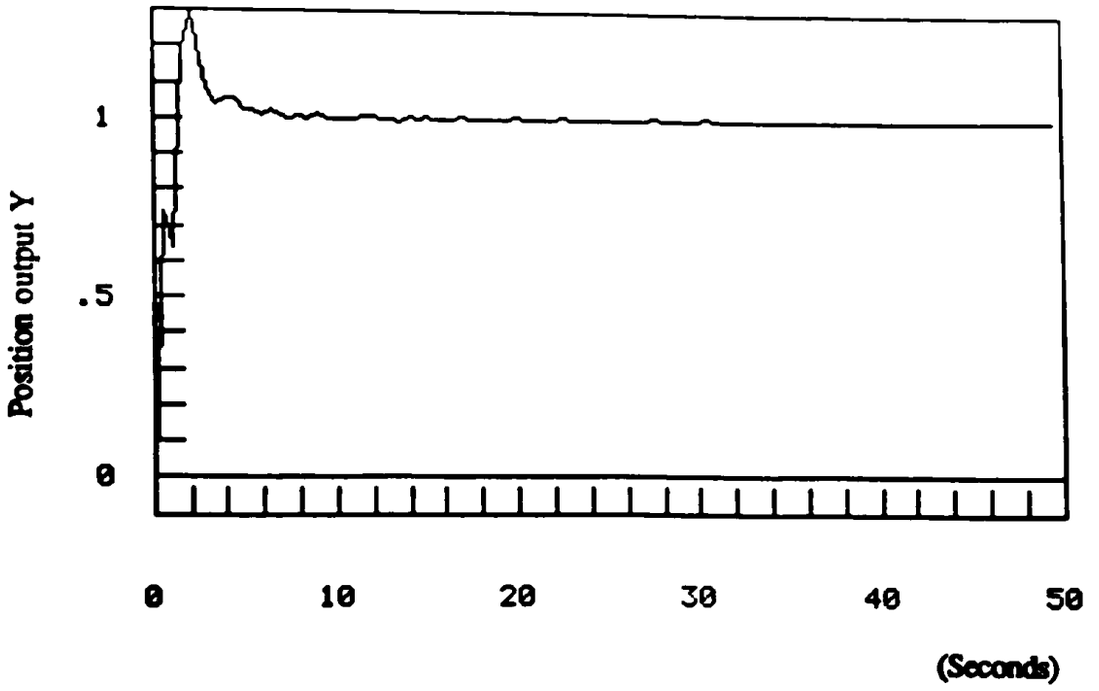

Fig. 3.12 Step response. Minimax design for the flexible beam with $x_j = 0$.

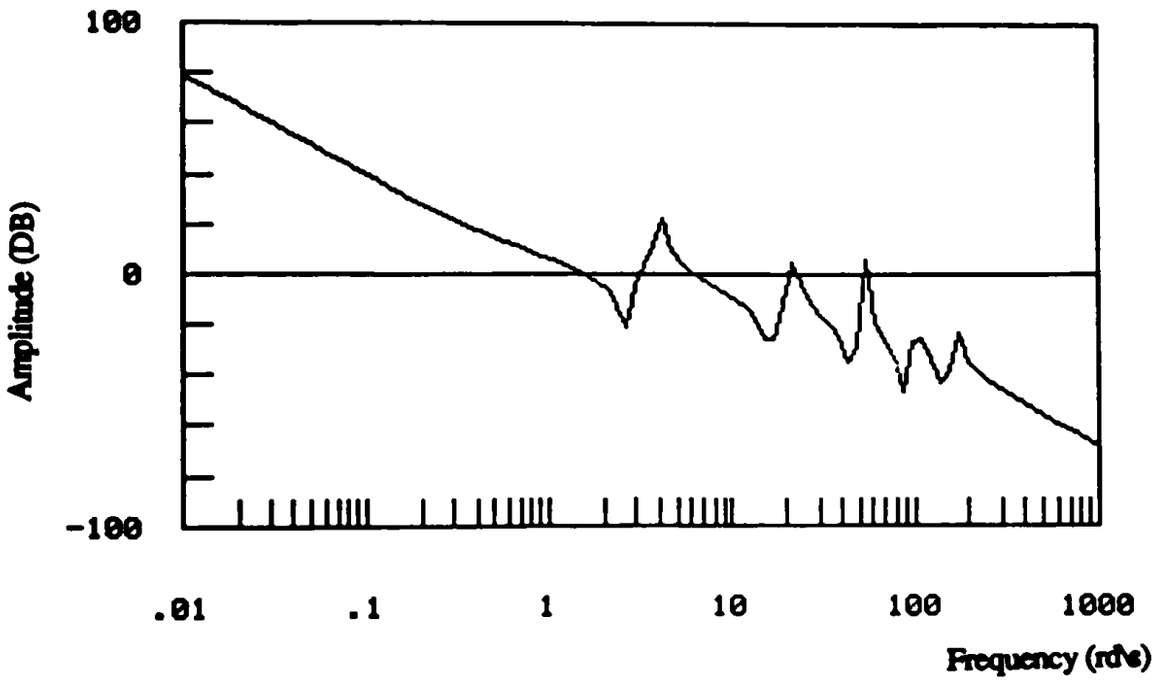

Fig. 3.13 Magnitude frequency response of the open-loop system GH(s). Minimax design.

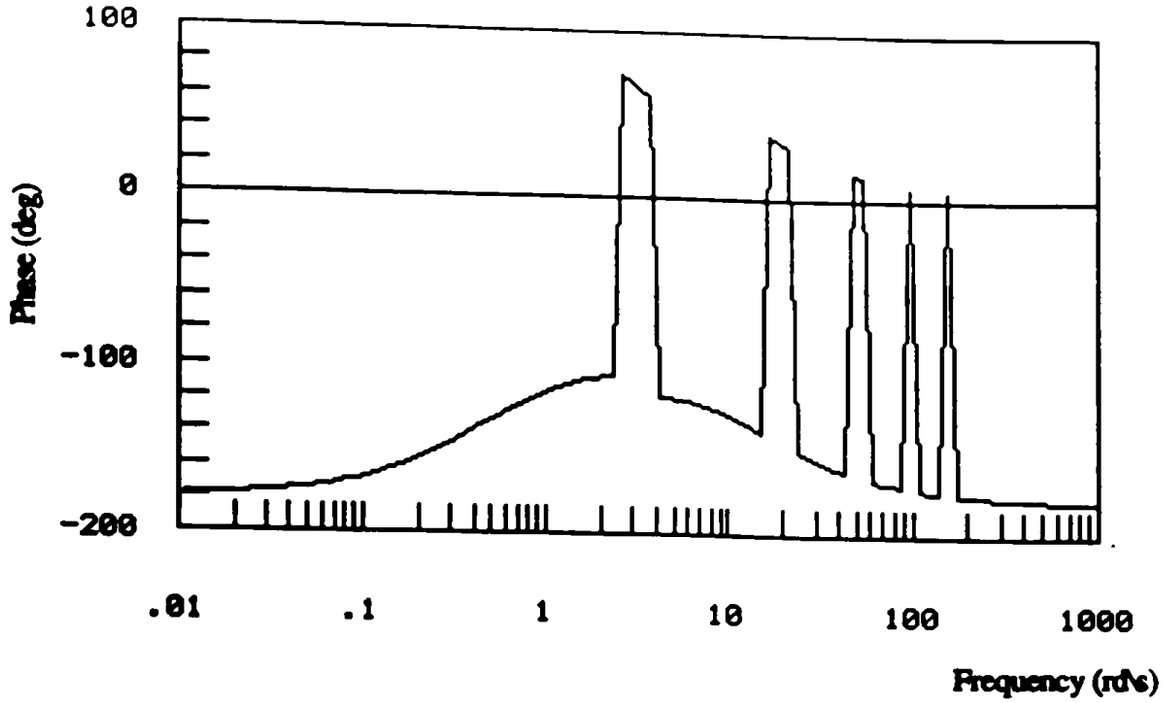

Fig. 3.14 Phase response of the open-loop system GH(s). Minimax design.

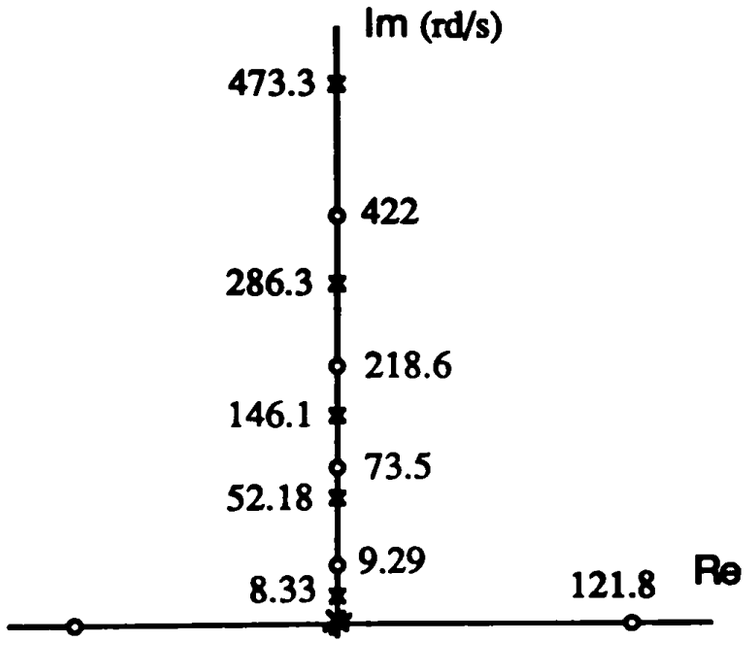

Fig. 3.15 Transfer function for a noncollocated placement of the actuator and the sensor.

Table 3.4 Minimax design for the plant of Fig. 3.15.
Nominal closed-loop system.

$\tau_1 = 1.5 \quad \tau_2 = 0.08$		$\tau_1 = 0.5 \quad \tau_2 = 0.07$	
minimax Compensator	Closed-loop poles	minimax Compensator	Closed-loop poles
$\lambda = .032$ $n_1 = 24.01$ $n_2 = 513.5$ $n_3 = -353.4$ $m_1 = -1975.9$ $m_2 = 3089.1$ $m_3 = 1220.7$ $m_4 = 347.2$	-.5 $-1.52 \pm j\ .31$ $-1.75 \pm j\ 6.24$ $-7.46 \pm j\ 5.68$ $-.83 \pm j\ 53.86$ $-.14 \pm j\ 146.9$ $-.034 \pm j\ 286.7$ $-.008 \pm j\ 473.5$	$\lambda = .117$ $n_1 = 19.5$ $n_2 = 290.2$ $n_3 = -666$ $m_1 = -960.6$ $m_2 = 4732.6$ $m_3 = 2465.3$ $m_4 = 1604.9$	-1.17 $-1.45 \pm j\ 2.18$ $-1.1 \pm j\ 6.6$ $-6.1 \pm j\ 4.7$ $-.4 \pm j\ 53.02$ $-.07 \pm j\ 146$ $-.016 \pm j\ 286.5$ $-.004 \pm j\ 473.4$

Table 3.5 Effect of model-parameter variations upon stability of closed-loop system

Closed-loop poles of compensated system under 30% decrease in all frequency modes of the evaluation model	
Minimax design ($\tau_1 = 1.5, \tau_2 = .08$)	State-space design
-.5 $-1.3 \pm j\ .5$ $-.06 \pm j\ 4.13$ $-8.5 \pm j\ 7.6$ $-1.5 \pm j\ 38.6$ $-.29 \pm j\ 103.4$ $-.07 \pm j\ 201$ $-.017 \pm j\ 331.6$	-.44 -5.79 $-.39 \pm j\ .46$ $+.17 \pm j\ 2.55$ $-2.09 \pm j\ 6.64$ $-.06 \pm j\ 39.1$ $-.008 \pm j\ 109.6$ $-.001 \pm j\ 214.7$ $-.0005$ v j 354

The pole-zero pattern of Fig. 3.16 describes the plant, for the first 5 elastic modes, of the 3 ft long aluminum flexible beam (Fig. 2.1) with a sensor located at x_j = 0.5 ft (from the actuator). In this case, the design of a stabilizing controller is not an easy task. The goal of this section is to address the problem of controlling this category of plants. We will first define a general class of systems which are characterized by a pattern of alternating poles and zeros on the imaginary axis. Then, we develop a robust low-order compensation method for the defined class of plants.

3.3.1 Statement of the problem

We consider a class of single-input, single-output systems which are characterized by zero damping and a pattern of interlacing poles and zeros as shown in Fig. 3.17.

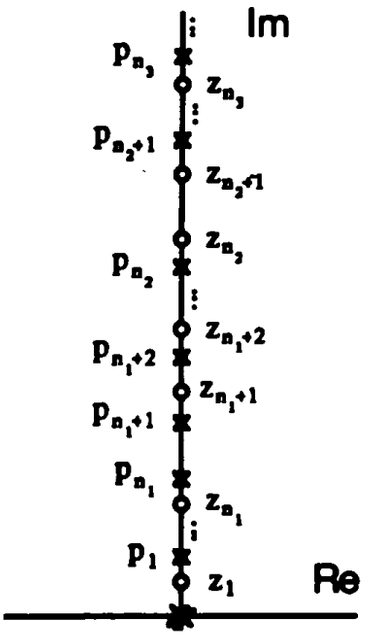

Fig. 3.17 Plant pole-zero locus

The pole-zero pattern of Fig. 3.16 describes the plant, for the first 5 elastic modes, of the 3 ft long aluminum flexible beam (Fig. 2.1) with a sensor located at x_j = 0.5 ft (from the actuator). In this case, the design of a stabilizing controller is not an easy task. The goal of this section is to address the problem of controlling this category of plants. We will first define a general class of systems which are characterized by a pattern of alternating poles and zeros on the imaginary axis. Then, we develop a robust low-order compensation method for the defined class of plants.

3.3.1 Statement of the problem

We consider a class of single-input, single-output systems which are characterized by zero damping and a pattern of interlacing poles and zeros as shown in Fig. 3.17.

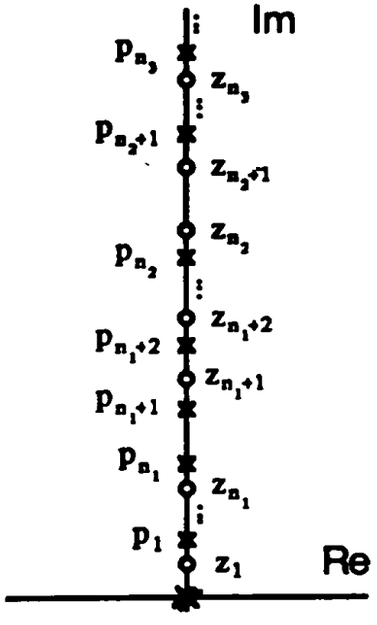

Fig. 3.17 Plant pole-zero locus

More specifically, the class of systems is defined by transfer functions of the following form

$$G(s) = \frac{Kg \prod_{k=1}^{n_1}(s^2+Z_k^2) \prod_{k=n_1+1}^{n_2}(s^2+Z_k^2) \ \dots \ \prod_{k=n_{r-1}+1}^{n_r}(s^2+Z_k^2)}{s^2 \prod_{k=1}^{n_1}(s^2+P_k^2) \prod_{k=n_1+1}^{n_2}(s^2+P_k^2) \ \dots \ \prod_{k=n_{r-1}+1}^{n_r}(s^2+P_k^2)} \qquad (3.38)$$

such that,

$$0 < n_1 < \dots < n_r$$

$$Kg > 0$$

$$P_i < P_{i+1}$$

$$Z_i < Z_{i+1} \quad \text{for } i = 0, \dots, n_r-1$$

and,

$$Z_k \in (P_{k-1}, P_k)$$

$$\text{for } k = n_j+1, \dots, n_{j+1}; \quad j = 0, 2, 4, \dots$$

$$Z_k \in (P_k, P_{k+1})$$

$$\text{for } k = n_j+1, \dots, n_{j+1}; \quad j = 1, 3, 5, \dots$$

A system in the class has n_r pairs of complex conjugate poles and zeros, all on the imaginary axis, in addition to a double pole at the origin (the rigid body mode). The n_r pairs of poles and zeros are assumed to be grouped into r subsets. Within each subset the poles and zeros have a regular alternating pattern, but from one subset to another, the alternating pattern is reversed. Thus, at the boundary of two subsets there are either two consecutive poles or zeros.

For these systems, classical compensation techniques, such as Bode, are not very useful due to the irregularities in interlacing. For example, it can be easily

demonstrated that a lead compensator produces an unstable design. One may use state-variable methods to produce a state-feedback observer type of controller. However, to ensure stability, the resulting controller could be of very high order, therefore very sensitive to modeling uncertainties. The H∞ approach to robust control may be one possible area of investigation, although some methods [27] do not handle plant poles and zeros on the imaginary axis. In this paper, we propose a compensation scheme for systems given by (3.38). The method is aimed at low-order and robust designs.

3.3.2 Generalized lead-lag compensators

The main result of this section is a compensation technique for systems (1). First, we define a notion called k-stability.

Definition 3.1

Consider an open-loop system G(s)

$$G(s) = K\, b(s)/a(s)$$

in a unity feedback closed-loop system, where $K > 0$, and a(s), b(s) are monic polynomials with deg(a) > deg(b). An open-loop pole P, that is $a(P) = 0$, is said to be k-stabilizable, if there exists a non empty interval $(0, K_0)$ such that the root locus originating from P is in the open left half plane for K in $(0, K_0)$. The closed loop system is said to be k-stable if every open-loop pole is k-stabilizable.

K-stability will be the goal that our compensation technique is aimed at. Obviously, a stable closed-loop system is not necessarily k-stable. In what follows we give three lemmas, which are the basis of the proposed compensation. The proofs of the lemmas are based on the classical root locus techniques [28]. The first lemma

departure angle of each branch. The departure angle x^i of the loci from the ith mode satisfies:

$$x^i = \theta - \alpha + \frac{\pi}{2}$$

where, θ and α are the phases of the pole and the zero of the lead compensator. Since for a lead compensator $0 < \theta - \alpha < \frac{\pi}{2}$, it is clear that branches from all the modes depart into the open LHP. Therefore, the system is k-stable.

Lemma 3.4

Consider a plant

$$G(s) = Kg \frac{\prod_{i=1}^{N-1}(s^2+Z_i^2)}{s^2\prod_{i=1}^{N-1}(s^2+P_i^2)}$$

where

$$Kg > 0$$

and

$$0< Z_i < P_i < Z_{i+1} \text{ for all } i \geq 1.$$

Let H(s) be a compensator given by

$$H(s) = K_h \frac{(s+Z)(s+Z^*)}{(s+P)(s+P^*)} \tag{3.39}$$

such that

$$K_h > 0,$$

$$0 < (\mathrm{Im}(P), \mathrm{Im}(Z)) < Z_1,$$

$$\mathrm{Re}(P) > \mathrm{Re}(Z) > 0$$

then all poles P_i of G(s), $i \geq 1$ are k-stabilizable.

Proof

The departure angle x^i of the loci from the pole P_i is given by:

$$x^i = \frac{\pi}{2} + (\alpha - \theta) + (\alpha^* - \theta^*)$$

where α , α^*, θ and θ^* are the phases of, respectively, Z, Z*, P and P*;
since, $0 < \alpha - \theta < \frac{\pi}{2}$, and $0 < \alpha^* - \theta^* < \frac{\pi}{2}$, then all branches from the poles P_i start in the open LHP, i.e. the poles P_i are k-stabilizable.

Lemma 3.5

Consider an open loop system

$$G(s) = Kg \frac{\prod_{i=1}^{N-1}(s^2+Z_i^2)}{s^2\prod_{i=1}^{N-1}(s^2+P_i^2)}$$

where

$$Kg > 0$$

and

$$0 < P_i < Z_i < P_{i+1} \text{ for all } i \geq 1.$$

Let H(s) be a compensator of the form

$$H(s) = K_h \frac{(s+Z)(s+Z^*)}{(s+P)(s+P^*)} \tag{3.40}$$

such that

$$K_h > 0,$$

$$0 < (\mathrm{Im}(P), \mathrm{Im}(Z)) < P_1$$

$$\mathrm{Re}(Z) > \mathrm{Re}(P) > 0$$

then, all poles P_i of G(s), $i \geq 1$ are k-stabilizable.

Proof

Again, we examine the departure angle x^i of the loci from the pole P_i. The phase x^i is given by:

$$x^i = -\frac{\pi}{2} - (\alpha - \theta) - (\alpha^* - \theta^*)$$

where α , α^*, θ and θ^* are the phases of, respectively, Z, Z*, P and P*;
since, $0 < \alpha - \theta < \frac{\pi}{2}$, and $0 < \alpha^* - \theta^* < \frac{\pi}{2}$, then all branches from the poles P_i start in the open LHP, i.e. the poles P_i can be k-stabilized.

It is to be noted that the lag compensator cannot stabilize the rigid body mode, i.e. the overall system is not k-stable. We shall call compensator (3.39) a generalized lead compensator, and compensator (3.40) a generalized lag compensator.

We now address the problem of stabilizing the class of systems (3.38). First, we note that to stabilize the rigid body mode, real lead compensation is necessary. Secondly, according to lemmas 3.4 and 3.5, each ith subset (i = 1, ..., r) of poles can be k-stabilized either by generalized lead or lag compensation (depending on interlacing). These observations suggest the compensator structure depicted in

Fig. 3.18. The real-valued lead pair (P_1^c, Z_1^c) is to stabilize the rigid body mode and the first set of poles (i = 1). A generalized lag pair (P_2^c, Z_2^c) is placed so that

$$P_{n_1} < (\mathrm{Im}(P_2^c), \mathrm{Im}(Z_2^c)) < P_{n_1+1}$$

and

$$\mathrm{Re}(Z_2^c) > \mathrm{Re}(P_2^c) > 0.$$

Both minimum and nonminimum phase configurations are possible, as shown in Figures 3.18 and Fig. 3.19. This special placement of (P_2^c, Z_2^c) provides the needed phase lag for the second set of poles (i = 2). Furthermore, it results in additional phase lead for the double integrator and the first set of poles. Next, notice the interlacing reversal between the second set (i = 2) and the third set (i = 3). Hence, a generalized lead pair (P_3^c, Z_3^c) is inserted so that

$$Z_{n_2} < (\mathrm{Im}(P_3^c), \mathrm{Im}(Z_3^c)) < Z_{n_2+1}$$

and

$$\mathrm{Re}(P_3^c) > \mathrm{Re}(Z_3^c) > 0.$$

This ensures the required phase lead for the third set (i = 3) of poles, and also introduces more phase lag to the second set of poles. Again, the generalized lead can be either minimum or nonminimum phase. The process can be continued in the same manner with a total of r pairs (P_i^c, Z_i^c), so that all the poles are k-stabilized.

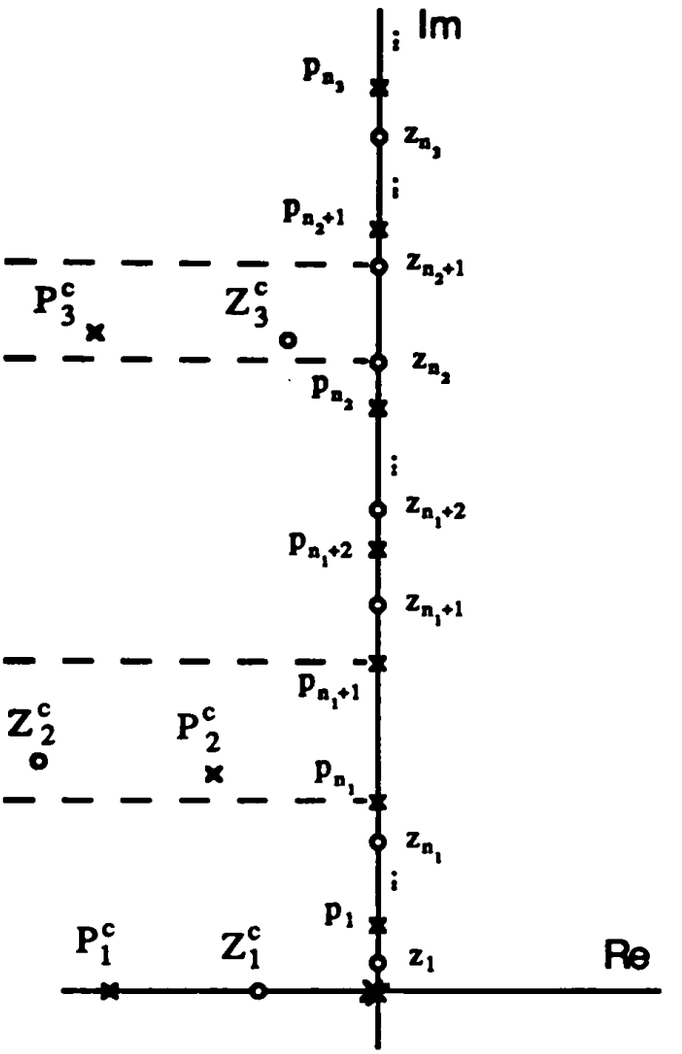

Fig. 3.18 Generalized lead-lag. Minimum-phase design.

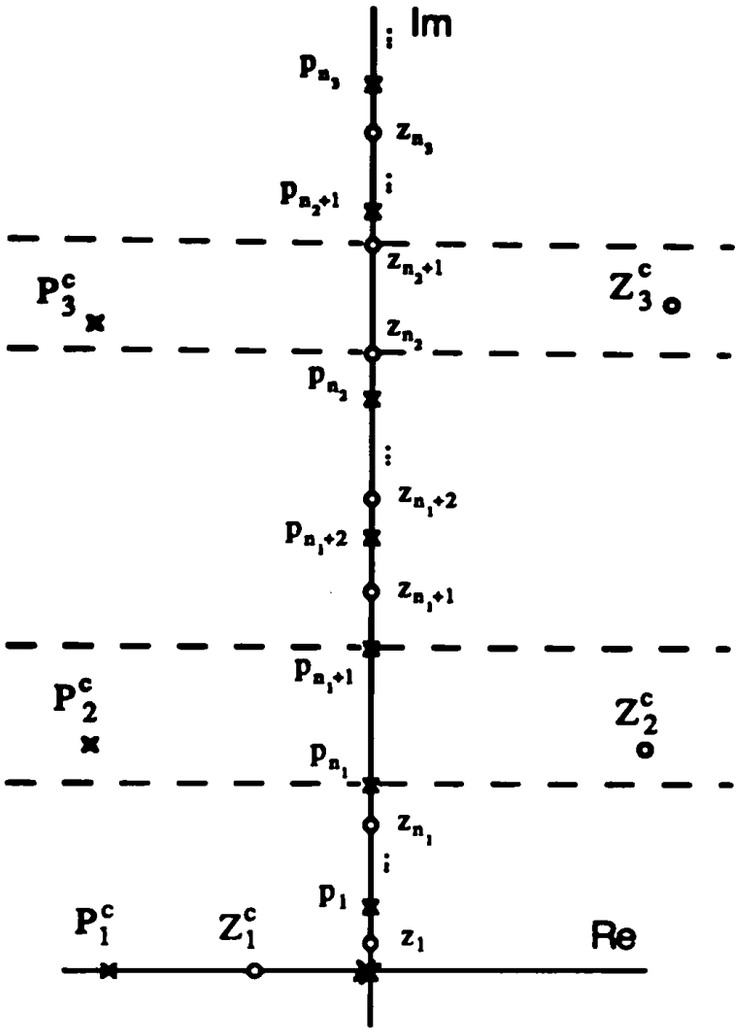

Fig. 3.19 Generalized lead-lag. Nonminimum design.

The following theorem gives necessary and sufficient conditions for the compensation procedure to be k-stable.

Let θ_i^j, i = 1, ..., r for j = 1, ..., n_r be the phase between Z_i^c and the plant pole P_j; α_i^j the phase between P_i^c and the pole P_j; x^j the departure angle of the loci branch that starts from P_j. We now state the main theorem.

Theorem 3.3

Let G(s) be a system given by (3.38). Let H(s) be a generalized lead-lag compensator defined by

$$H(s) = \frac{K_h\ (s+Z_1^c) \prod_{i=2}^{r} (s+Z_i^c)\ (s+Z_i^{c*})}{(s+P_1^c) \prod_{i=2}^{r} (s+P_i^c)\ (s+P_i^{c*})} \qquad (3.41)$$

such that

$$K_h > 0$$

$$P_1^c > Z_1^c > 0$$

$$P_{n_1} < (\mathrm{Im}(P_2^c), \mathrm{Im}(Z_2^c)) < P_{n_1+1}, \text{ and } \mathrm{Re}(Z_2^c) > \mathrm{Re}(P_2^c) > 0$$

$$Z_{n_2} < (\mathrm{Im}(P_3^c), \mathrm{Im}(Z_3^c)) < Z_{n_2+1}, \text{ and } \mathrm{Re}(P_3^c) > \mathrm{Re}(Z_3^c) > 0$$

$$P_{n_3} < (\mathrm{Im}(P_4^c), \mathrm{Im}(Z_4^c)) < P_{n_3+1}, \text{ and } \mathrm{Re}(Z_4^c) > \mathrm{Re}(P_4^c) > 0$$

$$\vdots$$

The unity feedback closed loop system is k-stable if and only if

1. Every pole P_k, $k = n_j + 1, \ldots, n_{j+1}$ for $j = 0, 2, 4, \ldots$ satisfies:

$$0 < \sum_{i=1}^{r} \theta_i^k - \alpha_i^k < \pi$$

2. Every pole P_k, $k = n_j + 1, \ldots, n_{j+1}$ for $j = 1, 3, 5, \ldots$ satisfies

$$-\pi < \sum_{i=1}^{r} \theta_i^k - \alpha_i^k < 0$$

Proof

The proof consists simply of examining the departure angles of each branch of the root locus. Let us consider the pole P_k , $k = n_j + 1, ..., n_{j+1}$ for $j = 0, 2, 4, ...$; the corresponding departure angle x^k is given by:

$$x^k = \frac{\pi}{2} + \sum_{i=1}^{r} \theta_i^k - \alpha_i^k$$

so, a sufficient condition for P_k to be k-stabilized is:

$$0 < \sum_{i=1}^{r} \theta_i^k - \alpha_i^k < \pi$$

In the same manner, if we consider the pole P_k , $k = n_j + 1, ..., n_{j+1}$ for $j = 1, 3, 5,...$

the departure angle x^k satisfies

$$x^k = -\frac{\pi}{2} + \sum_{i=1}^{r} \theta_i^k - \alpha_i^k$$

i.e., it suffices for P_k to be k-stabilized that:

$$-\pi < \sum_{i=1}^{r} \theta_i^k - \alpha_i^k < 0$$

it is obvious that the compensator poles P_i^c , $i = 1, ..., r$ are k-stabilizable, since they belong to the open LHP.

Now, we need to prove the k-stability of the rigid body mode. For this, we consider the loci branch that departs from the rigid body mode.

Let P_e be the closed loop pole that corresponds to a sufficiently small displacement from the point (0, 0) in the upper half of the complex plane.

Define α as the phase between P_e and (0, 0), and $(\theta_1^e - \alpha_1^e) > 0$ the phase contribution from the real lead pair (P_1^c , Z_1^c) at the pole P_e .

Let the angular contribution from any two symmetric zeros be ξ_i , where ξ_i are small positive numbers.

Let the phase contribution from any two symmetric poles be $-\varepsilon_i$, where ε_i are small positive numbers. Thus, the angle α is given by

$$\alpha = \frac{\pi}{2} + \frac{1}{2}\left((\theta_1^e - \alpha_1^e) + \sum_i (\xi_i - \varepsilon_i) \right)$$

for a small displacement the term $\sum_i (\xi_i - \varepsilon_i)$ is small, therefore it is possible to place the lead (P_1^c , Z_1^c) so that

$$(\theta_1^e - \alpha_1^e) >> \sum_i (\xi_i - \varepsilon_i) ,$$

i.e. the rigid body mode is k-stabilizable.

It is also clear that conditions 1 and 2 of theorem (3.3) are necessary. Since, any violation of conditions 1 and 2 of the theorem implies a loci branch departs in the open RHP. In this case the closed-loop system is not k-stable.

3.3.3 Design procedure

In this section we describe a procedure for selecting generalized lead-lag compensators for systems (3.38). A simple example is given to illustrate the design and to show the robust stability.

1. Start with some real-valued lead (P_1^c , Z_1^c). The zero Z_1^c should be close enough to the origin so that the rigid body mode can be k-stabilized. Some additional

phase lead will be introduced by (P_i^c , Z_i^c) $i \geq 2$, and should be taken into account for the k-stabilization of $P_1, ..., P_{n1}$.

2. Select a generalized lag (P_2^c, Z_2^c) to stabilize P_{n1+1} and P_{n2}, i.e. by satisfying condition 2 of theorem (3.3). The lag contribution can be increased by pulling P_2^c toward the imaginary axis and stretching Z_2^c to the left of the complex plane. If (P_i^c , Z_i^c) $i \geq 3$ will be required, then allow some additional phase lag. When P_{n1+1} and P_{n2} are k-stabilized, the poles P_{n1+2} , ..., P_{n2-1} are most probably k-stabilized (it is guaranteed under certain conditions). Nevertheless, the stability of every mode has to be checked (step 4). It is to be noted that the amount of damping may be controlled by the compensator gain K_h, and (or) by stretching the pair (P_2^c , Z_2^c) which results in a larger departure angle.

3. If higher order compensation (i.e. (P_i^c , Z_i^c) $i \geq 3$) is necessary , then repeat step 2 according to the pole-zero interlacing.

4. After the compensator is selected, one has to be check that all poles satisfy the k-stability conditions of the theorem. Finally, an appropriate compensator gain K_h is selected.

In figures 3.20 and 3.21 we show the shape of the root locus for the minimum-phase and nonminimum-phase design. For simplicity, the case r = 2 is considered, i.e. two sets of poles and zeros with one reversal in the pole-zero interlacing.

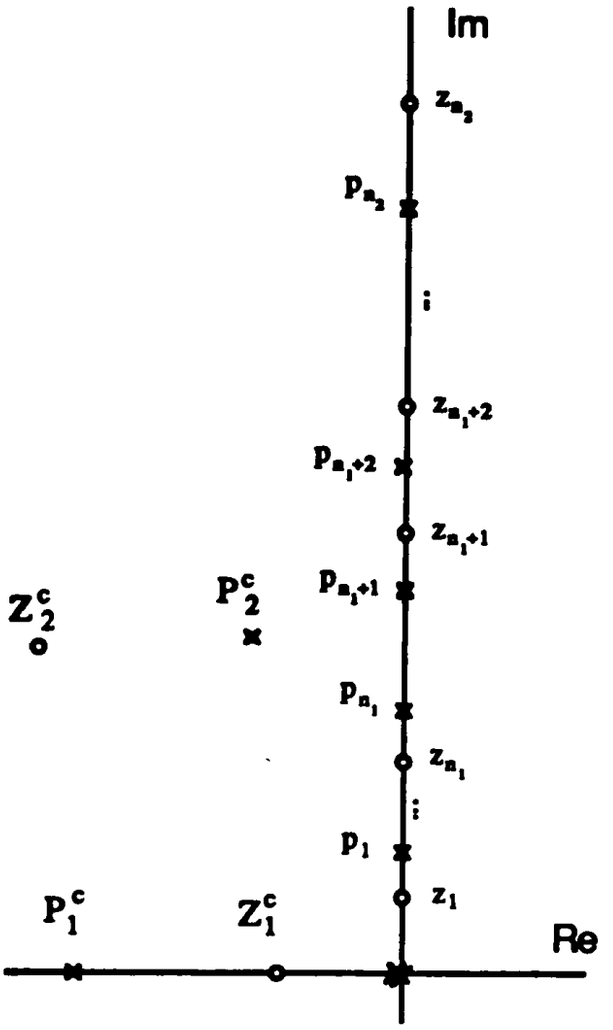

Fig. 3.20 Root-locus of the minimum-phase design.

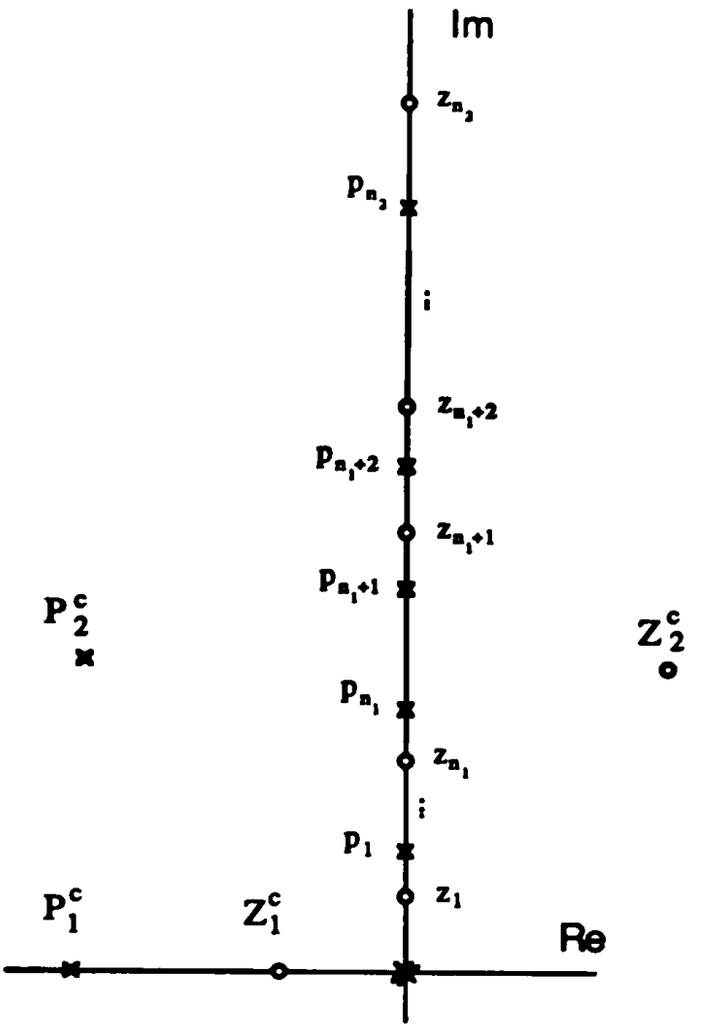

Fig. 3.21 Root-locus of the nonminimum-phase design.

Example 3.5: Noncollocated flexible beam control

To illustrate the proposed compensation technique, we consider the noncollocated control of the flexible beam depicted in Fig. 2.1, which has a transfer function as shown in Fig. 3.16. Following the procedure, a generalized lead-lag controller is found to be

$$H = K_h \frac{(s + 0.2)(s - 250 + j\,100)(s - 250 - j\,100)}{(s + 100)(s + 250 + j\,100)(s + 250 - j\,100)}$$

We then conducted simulation studies for $K_h = 100000$. Figures 3.22-3.25 show the Bode plots for the closed-loop and open-loop compensated system. Figures 3.26-

3.27 gives the Bode plots of the compensator H(s), and Fig. 3.28 shows the step response of the closed-loop system.

Again, to verify the robustness of the system we simulated the design with a 25% drop in the 5 flexibility modes of the evaluation model (Fig. 3.16). Table 3.6 gives the closed-loop poles for both the nominal and perturbed evaluation models. These results indicate a satisfactory performance with adequate robustness.

3.3.4 Conclusions

In this section we have presented a design methodology for a specific class of dynamical systems. The control synthesis is relatively simple and can provide a low-order and robust compensation for the high order plant. The method handles poles and zeros on the imaginary axis, which are in a pattern not easy to compensate for. An important application is flexible beam control when exact collocation cannot be achieved. There is a considerable amount of flexibility in the choice of the pole-zero topology of the compensator. Typically, several trials are required to obtain satisfactory damping for each mode.

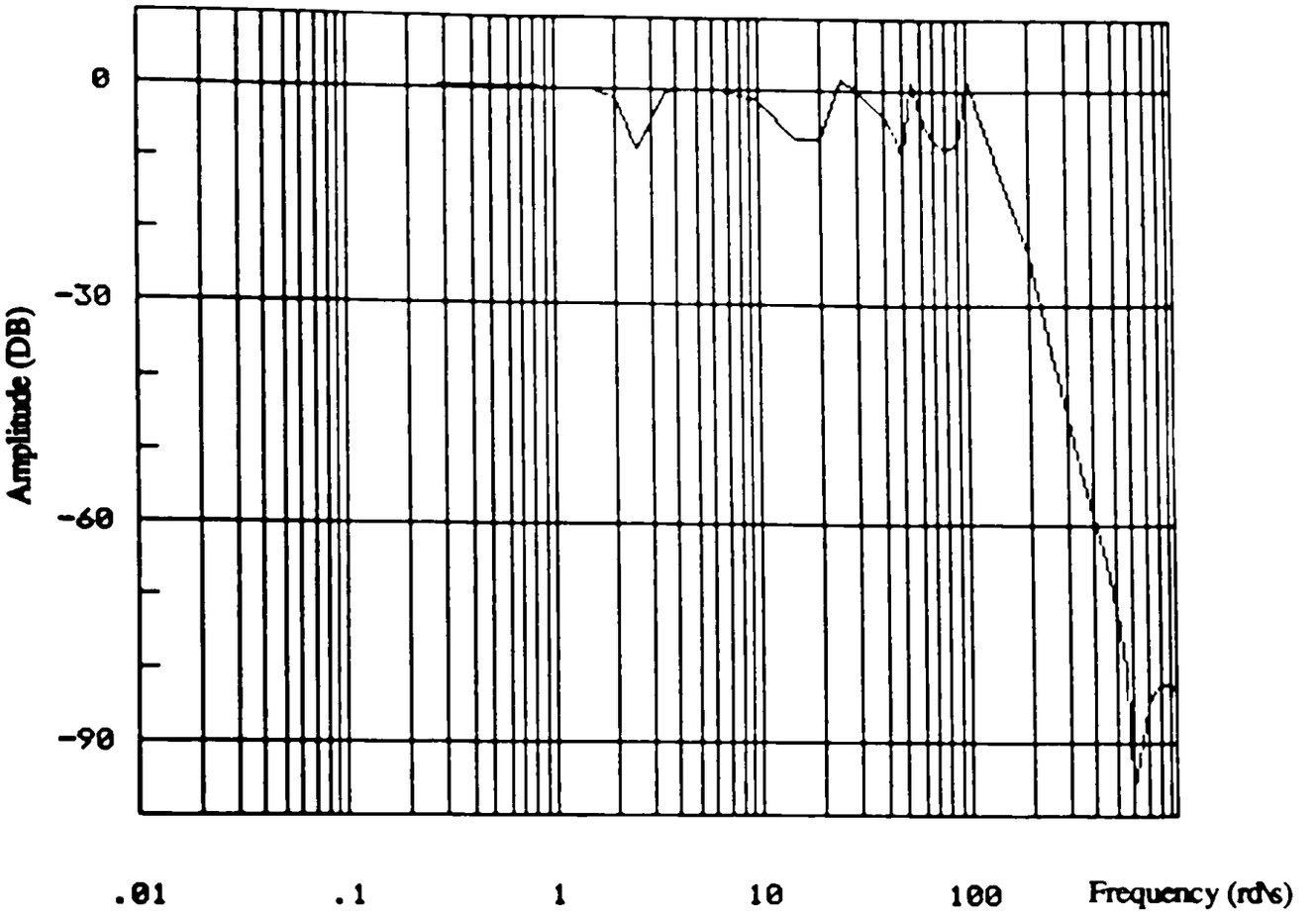

Fig. 3.22 Magnitude frequency response of the closed-loop system. Generalized lead-lag compensation.

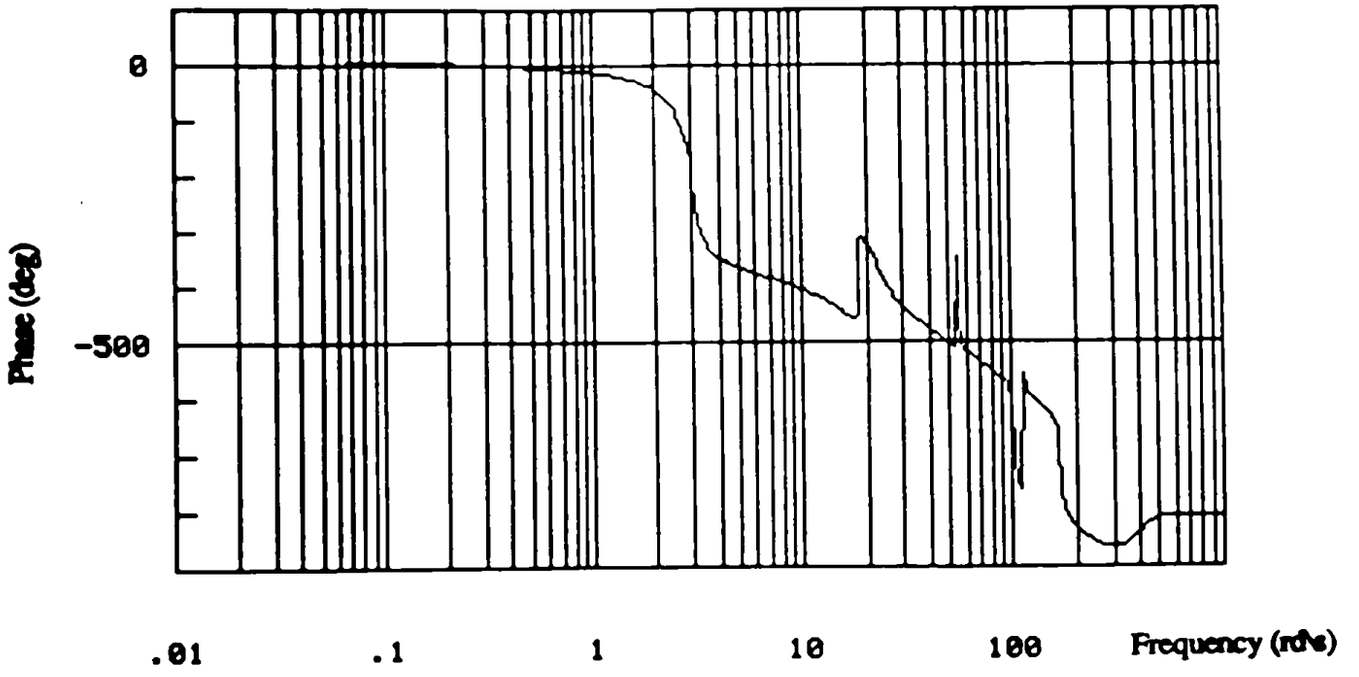

Fig. 3.23 Phase response of the closed-loop system. Generalized lead-lag compensation.

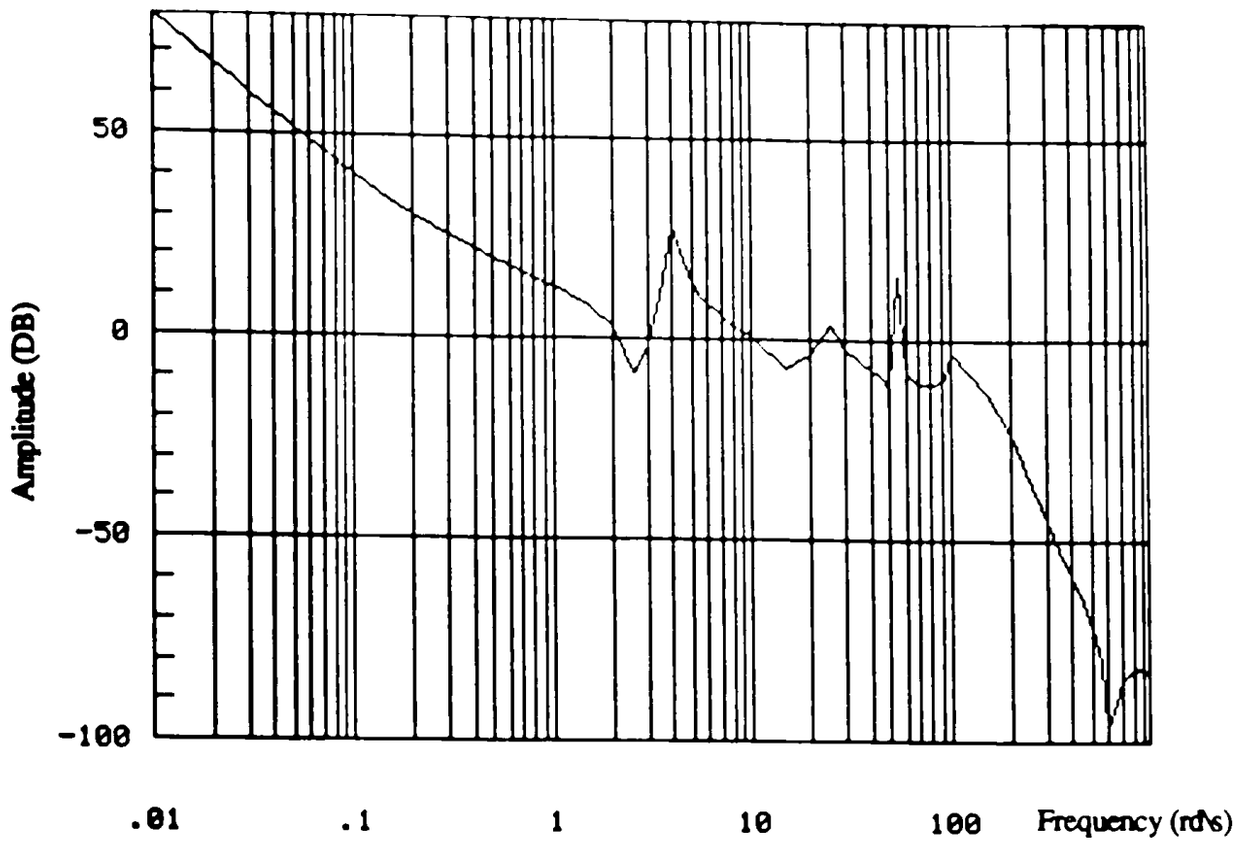

Fig. 3.24 Magnitude frequency response of the open-loop system GH(s). Generalized lead-lag compensation.

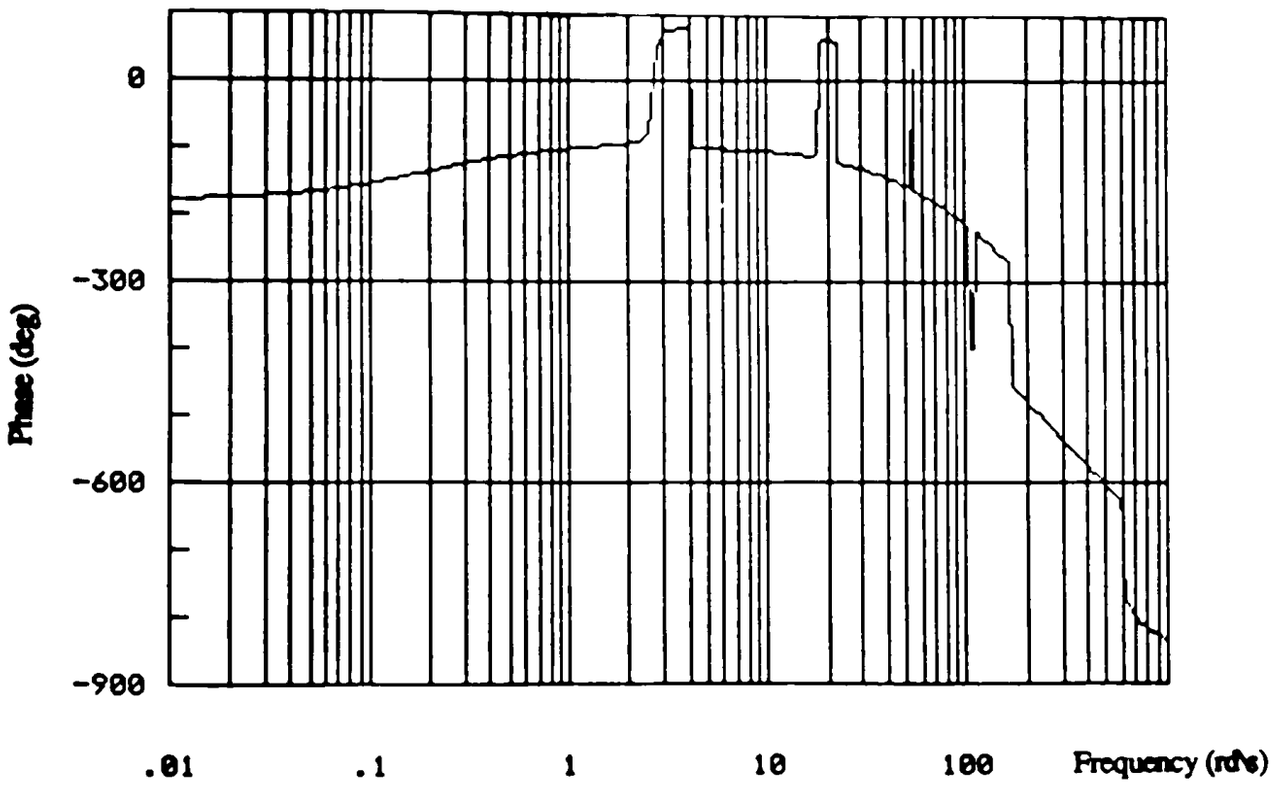

Fig. 3.25 Phase response of the open-loop system GH(s). Generalized lead-lag compensation.

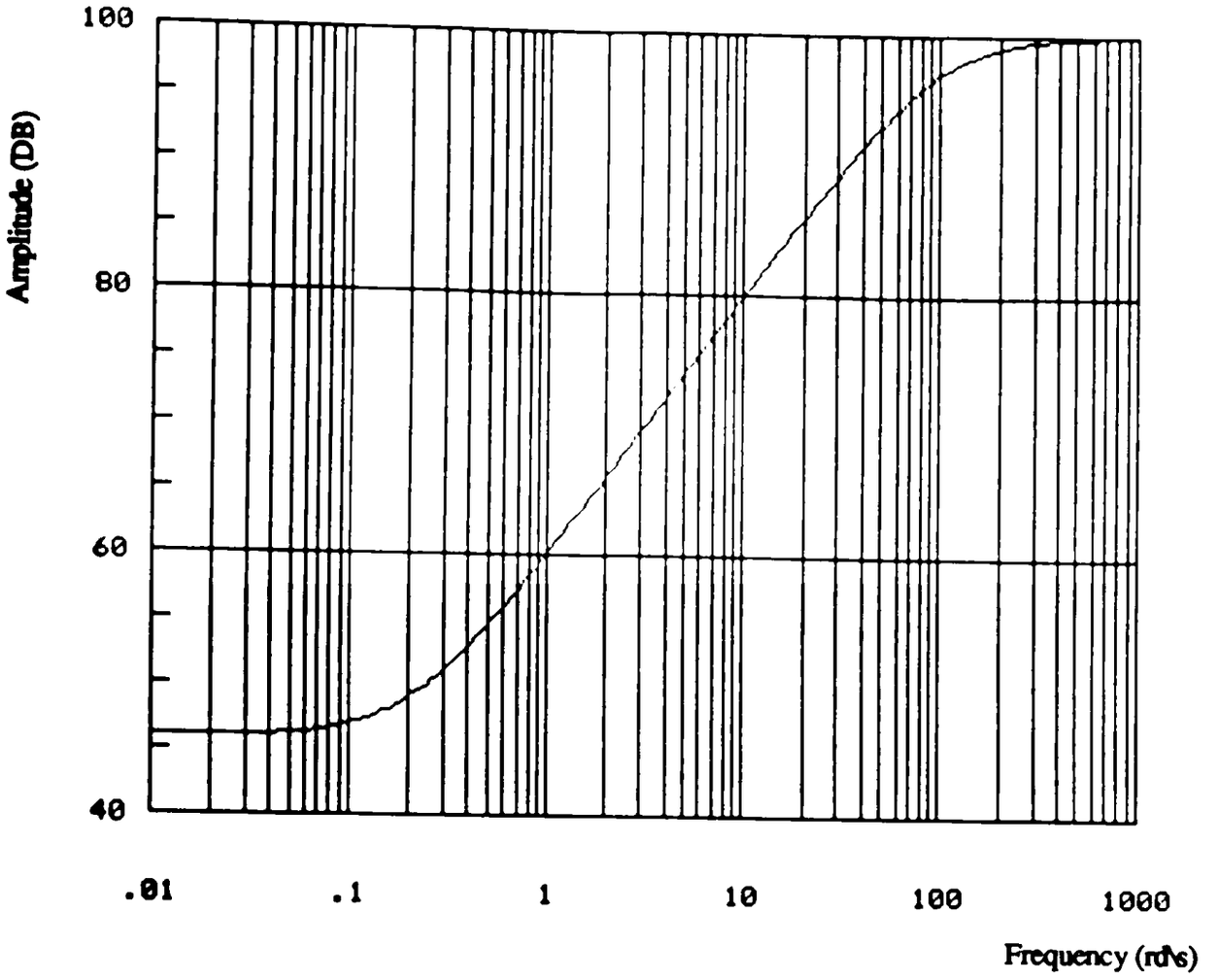

Fig. 3.26 Magnitude frequency response of the compensator H(s). Generalized lead-lag compensation.

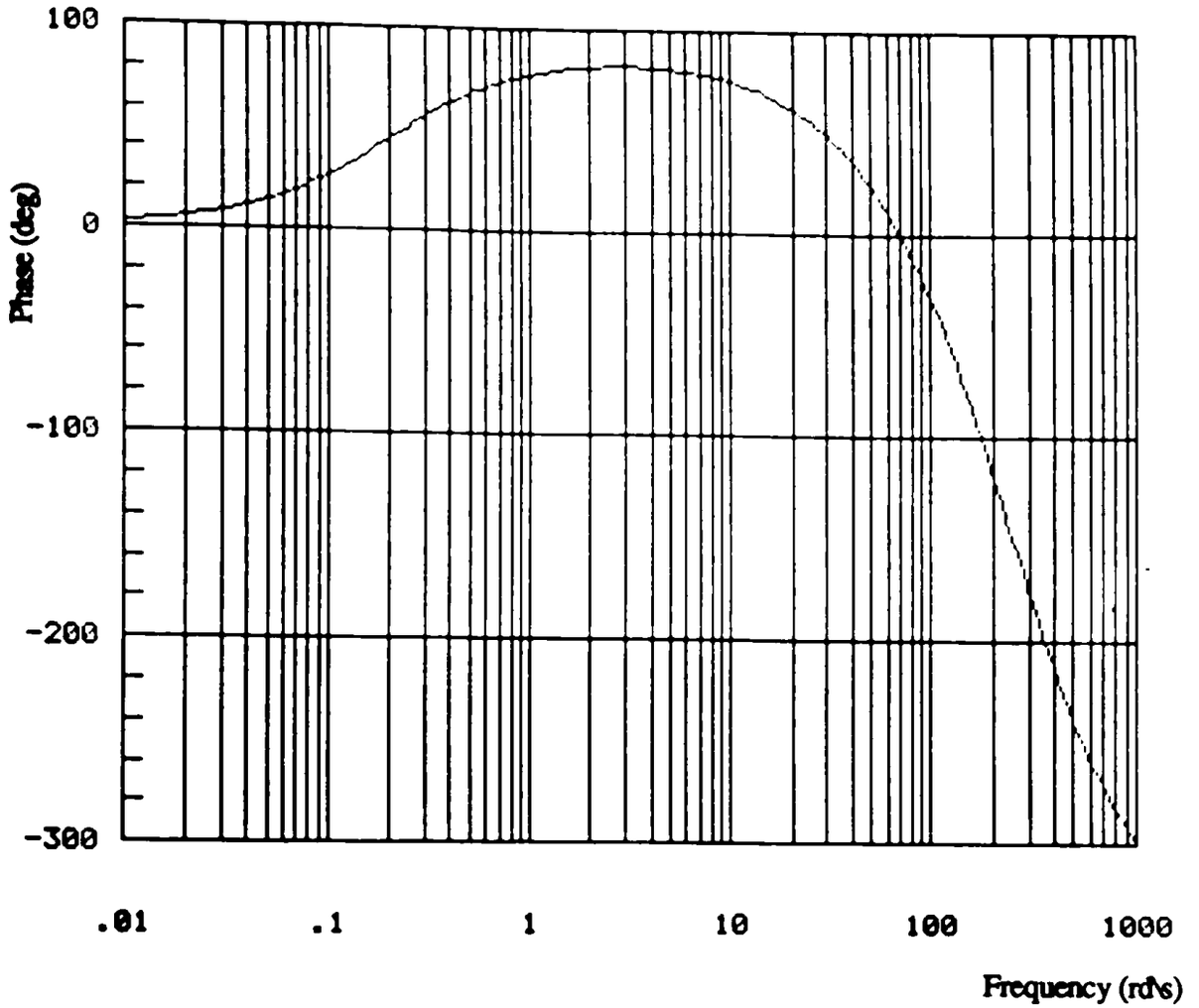

Fig. 3.27 Phase response of the compensator H(s). Generalized lead-lag compensation.

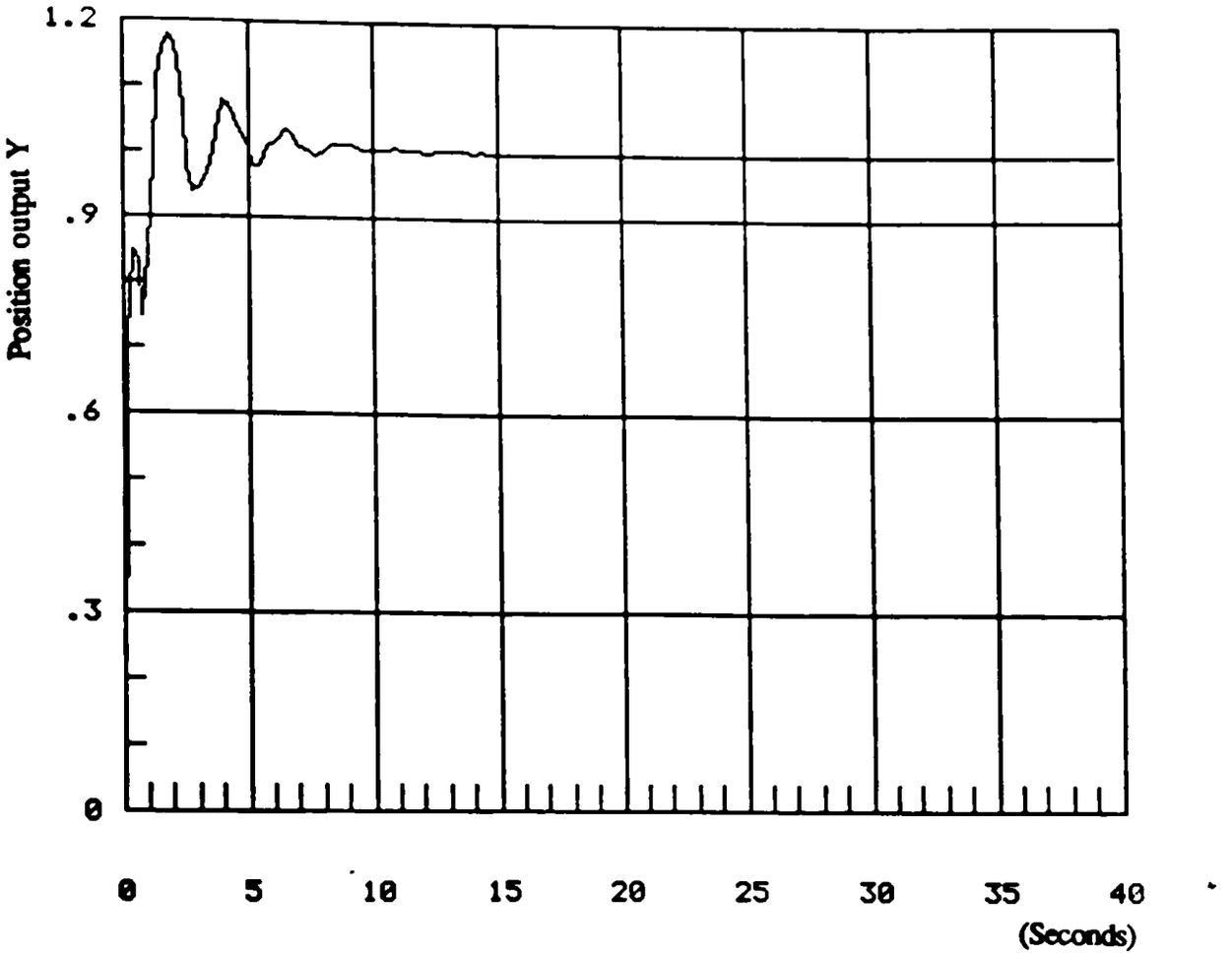

Fig. 3.28 Step response of the closed-loop design.
Generalized lead-lag compensation.

Table 3.6 Generalized lead-lag design for the flexible beam (x_j = 0.5ft).
Effect of parameter variations upon stability.

Closed-loop poles of compensated system	
Nominal system	25% decrease in frequency modes of evaluation model
-.209 -.47 ± j 2.69 - 4.1 ± j 21.6 - 30.1 ± j 5.9 -.33 ± j 55.6 - 1.1 ± j 101.3 - 3.4 ± j 169.5 - 260.5 ± j 106.9	-.24 ± j .2 -.32 ± j 3.1 -.28 ± j 16.8 -.03 ± j 41.2 -.02 ± j 76.8 - 95.8 -.34 ± j 126.6 - 250.8 ± j 100.5

CHAPTER IV

MULTIVARIABLE CONTROL OF FLEXIBLE STRUCTURES

The structural representation of a complex flexible structure can contain many 'clumped' low-frequency modes. Hence, there is a need to control a large number (say > 50) of elastic modes, which is well beyond the capacity of a SISO control logic. In this case, a MIMO design with multiple sensors and actuators is required, for mutivariable control can provide more advantages and versatility over SISO control. We also mention that many large structural systems are inherently multi-variable problems.

It is desirable to use the capabilities of MIMO control to achieve some special properties that enhance the control performance. The main question being asked in this chapter is what are the advantages offered by a multi-output design ? We give a partial answer to this question by showing that a multi-sensor design can greatly improve the robustness of the closed-loop system.

An important problem in LFS control is how to select, in some optimal sense, the locations (on the LFS) of a limited number of actuators and sensors. Some literature is available on the optimal sensor and/or actuator placement for flexible structures. Most of the methods consider a stochastic environment and assume Gaussian distributions for observation noise and input disturbances. The optimal selection of the locations is then determined by optimizing some appropriate cost functional. In [29], a standard LQG problem is considered, and the optimal placement is obtained by minimizing the cost functional with regard to these locations.

CHAPTER IV

MULTIVARIABLE CONTROL OF FLEXIBLE STRUCTURES

The structural representation of a complex flexible structure can contain many 'clumped' low-frequency modes. Hence, there is a need to control a large number (say > 50) of elastic modes, which is well beyond the capacity of a SISO control logic. In this case, a MIMO design with multiple sensors and actuators is required, for mutivariable control can provide more advantages and versatility over SISO control. We also mention that many large structural systems are inherently multi-variable problems.

It is desirable to use the capabilities of MIMO control to achieve some special properties that enhance the control performance. The main question being asked in this chapter is what are the advantages offered by a multi-output design ? We give a partial answer to this question by showing that a multi-sensor design can greatly improve the robustness of the closed-loop system.

An important problem in LFS control is how to select, in some optimal sense, the locations (on the LFS) of a limited number of actuators and sensors. Some literature is available on the optimal sensor and/or actuator placement for flexible structures. Most of the methods consider a stochastic environment and assume Gaussian distributions for observation noise and input disturbances. The optimal selection of the locations is then determined by optimizing some appropriate cost functional. In [29], a standard LQG problem is considered, and the optimal placement is obtained by minimizing the cost functional with regard to these locations.

In [30], a similar approach is proposed, and necessary and sufficient conditions for the existence of the optimal locations are stated.

Next, we consider the multi-output control problem of elastic systems. Our goal is to use the flexibility offered by a multivariable design to improve the system's robustness. This approach is motivated by the sizable parameter uncertainties that occur in the design models of LFS. A solution to this problem is obtained in the form of an optimal selection procedure of the sensor locations. The method achieves a robust control design and is based on the concept of eigenstructure assignment by orthogonal projections.

We have discussed in chapter III the model dependence on the spatial locations of the sensors (and actuators). This important property of flexible structures will also be used in section 4.1 to derive the optimal sensor placement algorithm.

Recall the FEM representation (2.2) of a flexible structure (of order k). In the following, we assume a state-space control design based on a truncated design model. The ROM has a dimension $n < k$ and is given by (2.27). The state-feedback control law and the state estimator are, respectively, as given by (2.29) and (2.30).

We now consider the problem of synthesizing a robust state observer. More specifically, our robustness design problem can be formulated as follows. We seek optimal sensor locations x_i (ie. an optimal matrix C (2.25)) and an optimal gain matrix L such that some robustness measure is minimized. In the subsequent section we examine the deterministic estimation problem by pole placement, based on the ROM. A quadratic cost is defined as a measure of robustness. This cost is first reduced by eigenstructure assignment, and is further minimized with respect to the sensor locations which yields the optimal selection of the locations.

4.1 Robust optimal sensor placement for flexible structures

In this section we examine the multivariable problem of designing a robust state estimator (2.30) by pole placement. We first discuss the problem of sensitivity to plant uncertainties and introduce a well-known measure of eigenvalue conditioning.

4.1.1 Eigenvalue conditioning

It is well-known, in the multi-input multi-output (MIMO) pole assignment problem, that for a given set of distinct eigenvalues, the gain matrix is not unique. This freedom of choice in the selection of the gain matrix should ideally be used to achieve some desirable properties in addition to satisfying eigenvalue placement constraints. For flexible structures, we intend to use this underdetermination to enhance the system robustness.

Consider the error dynamics of the asymptotic observer (2.31). Our objective is to choose matrices C and L such that the assigned eigenvalues of (A - LC) are the least sensitive to parameter variations in the model. It is well-known in numerical analysis [31] that eigenvalue sensitivity depends on the condition number of the eigenvector matrix. More precisely, let λ_i be a distinct eigenvalue and f_i , z_i be the corresponding right and left eigenvectors of a given matrix. The eigenvalue condition number, which is a measure of eigenvalue sensitivity, is defined as

$$\mathrm{Cond}_i(\lambda_i) = \frac{\|f_i\|_2 \, \|z_i\|_2}{|z_i^t f_i|} \geq 1. \qquad (4.1)$$

Let $F = (f_1, ..., f_n)$ be the eigenvector matrix. It is shown in [31] that

---

† The 2-norm of a vector $v = (v_i)$ is $\|v\|_2 = (\sum_{i=1}^{n} v_i^2)^{1/2}$.

$$\max_i \text{Cond}_i \leq K_2(F) = \|F\|_2 \|F^{-1}\|_{2\dagger\dagger} \geq 1 \qquad (4.2)$$

where, $K_2(F)$ is defined to be the condition number of the matrix F. Equation (4.2) indicates that $K_2(F)$ can represent a measure of eigenvalue sensitivity, or equivalently, of robustness. Therefore, for the least sensitivity, $K_2(F)$ should be minimized. Moreover, a perfect conditioning, ie. best robustness, is achieved when the matrix F is orthogonal ($K_2(F) = 1$).

Eigenstructure assignment in multivariable linear systems has in the last years been applied to robust control design. For example, in [32, 33], a scalar index is defined based on the condition number (4.1), and a constrained optimization of the index is performed. The constraints are pole assignment requirements which are expressed as Sylvester's equations. Kautsky [34] defines equivalent measures of robustness which are all related to (4.1). Then, orthogonal projections into the linear space of eigenvectors are performed to reduce the sensitivity measures. This method is based on the QR decomposition and is numerically reliable and efficient. Juang [35] follows the same approach to minimize a quadratic robustness index, utilizing the singular value decomposition (SVD). Next, we apply this method of orthogonal projections to develop a robust sensor placement procedure for flexible structures.

4.1.2 Robust optimal sensor placement

Consider the problem of allocating arbitrary and distinct eigenvalues $\Lambda = \{\lambda_i\}_{i=1}^n$ to the matrix (A - LC). It is well-established that a solution exists if and only if (A, C) is observable. Moreover, in the MIMO case, the associated eigenvector matrix $F = \{f_i\}_{i=1}^n$ of rank n is not unique [36] (and so is the gain matrix L). More precisely, the eigenvector f_i belongs to a linear subspace of rank m ($m < n$). It is also shown in [36] that the eigenvector matrix can be partially assigned, and that a gain

---

†† The 2-norm of a matrix $A = (a_{ij})$ is (maximum eigenvalue of $A^t A)^{1/2}$.

matrix can be uniquely determined by specifying an eigenstructure. The method presented in [34, 35], for robust eigenstructure assignment, consists of determining eigenvectors f_i which are as 'orthogonal' as possible. The eigenvectors are selected such that the matrix F is a least-square approximation of a given orthonormal matrix. Based on this approach, we define a quadratic robustness index as in [35].

Definition 4.1

Suppose (A, C) is observable, and let L be the (n x m) gain matrix that assigns arbitrary and distinct eigenvalues $\Lambda = \{\lambda_i\}_{i=1}^n$. Let $\mathcal{F} = \{F = \{f_i\}_{i=1}^n\}$ be the set of all eigenvector matrices associated with the eigenvalues Λ. Suppose Q is a given n-dimensional set of orthonormal vectors. We define a quadratic cost functional J as

$$J = \|F - Q\|_f^2 \dagger$$

where $F \in \mathcal{F}$.

The minimization of the index J is the basis for the selection of a well-conditioned eigenvector matrix F. More specifically, the following theorem holds.

Theorem 4.1

Suppose $\|F - Q\|_2 < 1$. Then minimizing the cost J, for $F \in \mathcal{F}$, reduces the condition number $K_2(F)$.

Proof

If (A, C) is observable, any set of distinct eigenvalues $\Lambda = \{\lambda_i\}_{i=1}^n$ can be assigned. Furthermore, since the eigenvalues are distinct, there exists at least one set of n linearly independent eigenvectors $F = \{f_i\}_{i=1}^n \in \mathcal{F}$ associated with Λ. Let Q =

---

† The f-norm of a matrix $A = (a_{ij})$ is $\|A\|_f = (\sum_{j=1}^{n}\sum_{i=1}^{n}|a_{ij}|^2)^{1/2}$.

$\{q_i\}$ be a set of n-dimensional orthonormal vectors, which implies $K_2(Q) = 1$. The cost J can be put in the form

$$J = \|F - Q\|_f^2 = \text{tr}\,[(F - Q)(F - Q)^t] \tag{4.3}$$

ie.,

$$J = \sum_{i=1}^{n}(f_i^t f_i - 2\, q_i^t f_i) + n \tag{4.4}$$

Next, we show that by minimizing (4.4), the condition number $K_2(F) = \|F\|_2 \|F^{-1}\|_2$ is reduced.

a) Ler $R = Q - F$ be the residual matrix. Hence, $\|F\|_2 \leq 1 + \|R\|_2$; which implies minimizing J decreases the 2-norm of F, $\|F\|_2$.

b) It is clear that $Q^t F = I - Q^t R$, and since F^{-1} exists, thus

$$\|F^{-1}\|_2 = \|F^{-1}\, Q\|_2 = \left\|(I - Q^t R)^{-1}\right\|_2$$

it is shown in [26] that if $\left\|Q^t R\right\|_2 = \|R\|_2 < 1$, then $(I - Q^t R)^{-1}$ exists and,

$$\|F^{-1}\|_2 = \left\|(I - Q^t R)^{-1}\right\|_2 \leq \frac{1}{1 - \left\|Q^t R\right\|_2} = \frac{1}{1 - \|R\|_2} \tag{4.5}$$

hence, if $\|R\|_2 < 1$, the RHS of (2.3) is minimum for $\|R\|_2 = 0$. Moreover, $\|R\|_2 \leq \|R\|_F$. Therefore, if $\|R\|_2 < 1$, minimizing J reduces the 2 norm of F^{-1}, ie. decreases $K_2(F)$. □

It should be noted that $\|R\|_2 < 1$ is a sufficient condition for reducing $K_2(F)$. However, an example can be given where $\|R\|_2 > 1$ and minimizing J deteriorates the condition number.

Theorem 4.1 shows that by minimizing the cost J, the condition number $K_2(F)$ of the eigenproblem is reduced. We now use the model dependence on the

sensor locations to further minimize $K_2(F)$ and derive a robust sensor placement for flexible structures.

Theorem 4.2

Given a n-dimensional orthonormal set $Q = \{q_i\}$, the optimum eigenvectors f_i^*, for system (2.27), that minimize the cost J are given by

$$f_i^* = (\lambda_i I - A^t)^{-1} C^t [C \Psi_i^t \Psi_i C^t]^{-1} C \Psi_i^t q_i$$

and the minimum cost J^* is

$$J^* = - \sum_{i=1}^{n} q_i^t \Psi_i C^t [C \Psi_i^t \Psi_i C^t]^{-1} C \Psi_i^t q_i + n \qquad (4.6)$$

with $\Psi_i = (\lambda_i I - A^t)^{-1}$. Furthermore, the optimal sensor locations that minimize J^* are solution of the minimization problem

$$\min_S J^* \qquad S \in \Omega \qquad (4.7)$$

where $S = (x_1, ..., x_m)$ is the sensor location vector , and Ω is the domain of all possible sensor locations on the structure.

Proof

Suppose (A-LC) has n distinct eigenvalues $\{\lambda_i\}$ and a set of eigenvectors F_A. In this case, it is easy to see that the dual $(A^t - C^t L^t)$ has the same eigenvalues $\{\lambda_i\}$, and a set of right eigenvectors $F = F_A^{-t}$. In addition, the condition numbers of F_A and F are identical, ie. $K_2(F_A) = K_2(F)$. Therefore, for convenience, we consider the dual $(A^t - C^t L^t)$ with eigenvalues $\{\lambda_i\}$ and a set of eigenvectors $F = \{f_i\}$. It is shown in [36] that

$$f_i = (\lambda_i I - A^t)^{-1} C^t u_i \tag{4.8}$$

for some u_i, ie. f_i belongs to the range of $(\lambda_i I - A^t)^{-1} C^t$. Let $\Psi_i = (\lambda_i I - A^t)^{-1}$, then the cost (3.2) becomes

$$J = \sum_{i=1}^{n} u_i^t C \Psi_i^t \Psi_i C^t u_i - 2 q_i^t \Psi_i C^t u_i + n. \tag{4.9}$$

The optimal u_i^* can be found from

$$\frac{\partial J}{\partial u_i} = 0$$

as

$$u_i^* = [C \Psi_i^t \Psi_i C^t]^{-1} C \Psi_i^t q_i \tag{4.10}$$

ie. the optimum eigenvectors f_i^* that minimize the cost J are

$$f_i^* = (\lambda_i I - A^t)^{-1} C^t [C \Psi_i^t \Psi_i C^t]^{-1} C \Psi_i^t q_i$$

substituting u_i^* in (4.9) results in

$$J^* = - \sum_{i=1}^{n} q_i^t \Psi_i C^t [C \Psi_i^t \Psi_i C^t]^{-1} C \Psi_i^t q_i + n \tag{4.11}$$

where, the output matrix C(S) is function of the sensor location vector S. The cost J^* can be further minimized by finding a minimizer S^* of (4.11). In other words, optimal sensor locations which minimizes the index J^* can be obtained by solving

$$\begin{aligned} &\min_S J^* \\ &S \in \Omega \end{aligned} \tag{4.12}$$

given Q orthonormal, and where Ω is the domain of all possible sensor locations on the structure. □

From the previous theoretical results, a design procedure for robust optimal sensor placement can be implemented. The sequential algorithm consists of five steps and can be summarized as follows.

4.1.3 Design procedure

1. Given desired distinct eigenvalues $\{\lambda_i\}$, start with an arbitrary sensor placement S, which results in a corresponding pair (A, C(S)).

2. Determine an eigenvector set $F^1 = \{f_i^1\}$ for (A^t, C^t), with condition number $K_2(F^1)$, and such that $f_i^1 \in R(\Psi_i C^t)$.

3. Construct an orthonormal set Q from F^1 (eg., by Gramm-shmidt orthogonalization).

4. Minimize J^* (4.7) to determine the optimal sensor locations S^* that results in a new pair (A, $C(S^*)$).

5. Given q_i ; compute u_i^* , the optimal eigenvector matrix F^*, and its condition number $K_2(F^*)$. The optimal gain matrix is, then, given by

$$L^t = - [u_1^* \dots u_n^*] F^{*-1} . \tag{4.13}$$

Remarks

The cost J^* as given by (4.6) is nonlinear. In fact, (4.7) is a constrained optimization problem, and it is very unlikely that it has a closed-form solution. A numerical solution, however, can be obtained. We also mention that the optimal

solution is dependent on the arbitrarily chosen orthonormal set Q. That is, the robustness of the solution can be affected by the choice of the matrix Q.

4.2 Design example: Flexible beam control

We applied the above procedure to control a three-foot long flexible aluminum beam, as shown in Fig. 2.1. The ROM is of order 4 and includes a rigid-body mode and the first elastic mode. The control consists of a controller-observer type of structure with one actuator, one position and one rate sensors. In step 1 of the design procedure, arbitrary sensor locations are set as $x_1 = 0.2$ ft. for position sensing, and $x_2 = 0.4$ ft. for velocity sensing. A set F^1 of eigenvectors is constructed (step 2) with a condition number $K_2(F^1) = 2541.4$. In step 4, the optimal sensor locations are found to be $x_1 = 3$ ft. and $x_2 = 0$ft. The resulting condition number of the optimal eigenvector matrix is $K_2(F^*) = 18.54$, which indicates the improvement in robustness.

Computer simulations were then conducted to test the control design. The evaluation model is of order 12 (rigid body and 5 flexible modes) to include the effect of the unmodeled higher-frequency dynamics. Table 4.1 gives the poles of the closed-loop nominal system. Figures 4.1 and 4.2 show the position y_1 and velocity y_2 outputs to a step command. Table 4.2 shows the effect of plant uncertainties upon the stability of the closed-loop system. To simulate the model-parameter variations, all the frequency modes in the evaluation model are lowered by 35%. Table 4.2 gives comparative results for a state-space SISO design with a collocated sensor and actuator, a SIMO design with arbitrary locations $x_1 = 0.2$ ft. and $x_2 = 0.4$ ft., and the SIMO design with optimal sensor locations $x_1 = 3$ft. and $x_2 = 0.$ft. In all three cases, the assigned sets of controller and observer eigenvalues are the same. Note the

better robustness of the optimal design, which is the only one that remains stable under the simulated plant uncertainties.

4.3 Conclusions

We have presented an optimal sensor placement method for robust control of flexible structures. The optimization is performed by minimizing a time-domain measure of robustness, and also uses the fact that the output-measurement matrix is function of the location of the sensors. In the multi-input multi-output case, by duality, the same approach can be applied to robust optimal placement of the actuators on the structure.

Table 4.1. Poles of the closed-loop system with a nominal evaluation model.

Closed-loop poles of the compensated system with a nominal evaluation model
- 1.03 - 1.35 - 2.36 - 3.445 - .976 ± j 1.02 - .3.07 ± j 3.186 - .46 ± j 23.06 - .103 ± j 55.32 - .029 ± j 102.8 - .02 ± j 169.35

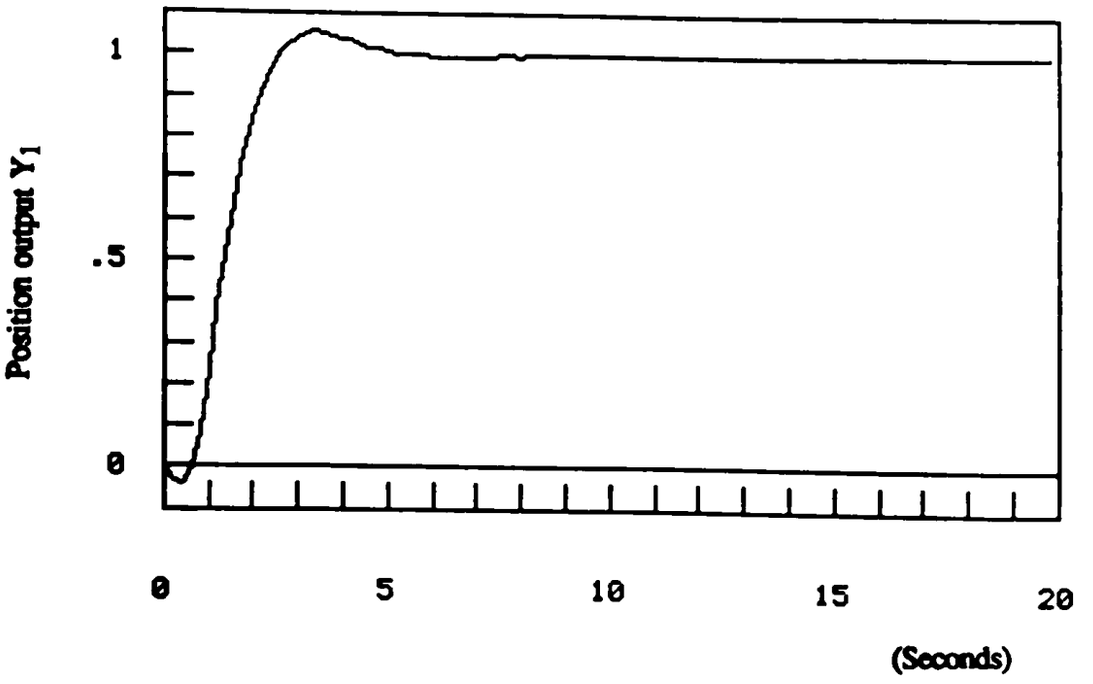

Fig. 4.1 Step response. Position output y_1 with the optimal sensor placement.

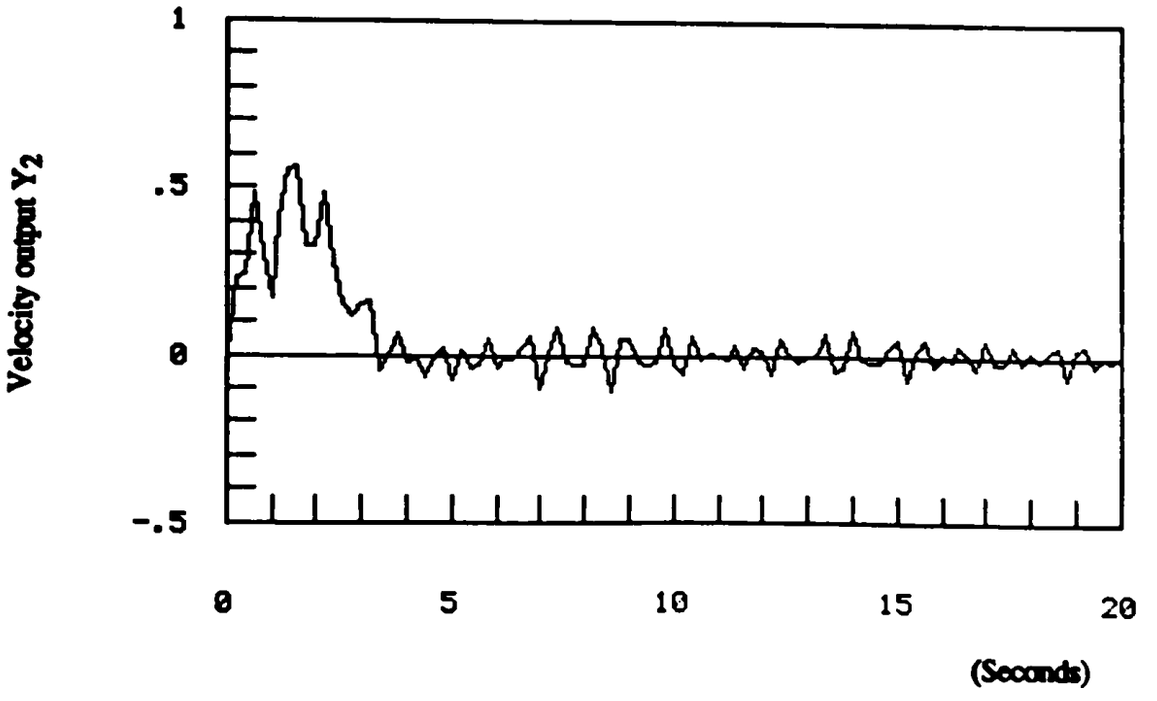

Fig. 4.2 Step response. Velocity output y_2 with the optimal sensor placement.

Table 4.2. Effect of model-parameter variations upon stability of closed-loop system.

Closed-loop poles of compensated system under 35% decrease in all frequency modes of the evaluation model		
SISO design (collocated)	SIMO design $x_1 = 0.2$ft, $x_2 = 0.4$ft	Optimal SIMO design $x_1^* = 3$ ft, $x_2^* = 0$ft
- .488	- .49	- .802
- 9.946	- 9.71	- 3.27
- .327 ± j .539	- .328 ± j .54	- .812 ± j .442
+ . 453 ± j 1.68	+ . 451 ± j 1.68	- .0163 ± j 1.414
- 3.81 ± j 4.31	- 3.89 ± j 4.33	- 4.64 ± j 4.005
+ .055 ± j 14.82	+ .045 ± j 14.81	- .89 ± j 15.49
+ .064 ± j 35.73	+ .053 ± j 35.73	- .237 ± j 36.3
+ .023 ± j 66.68	+ .016 ± j 66.68	- .068 ± j 67.06
+ .014 ± j 109.9	+ .007 ± j 109.9	- .047 ± j 110.3

CHAPTER V

CONCLUSION

A Large flexible structure is usually described by an approximate finite model of very high-order. This model includes a considerable number of elastic modes that are of low-frequency, very lightly damped and closely clustered. Furthermore, due to the modeling approximations involved, significant uncertainties in the model parameters are present. Therefore, the basic problems in LFS control are high dimensionality and model uncertainties.

In the control of structural systems, there are other considerations than just providing additional damping to the open-loop poles. In particular, by placing sensors and actuators on the structure, it is the overall input/output transfer function that is affected with each actuator/sensor configuration. We have demonstrated, for a class of elastic systems, an interesting pattern of movement of the plant zeros as a function of the sensor location. It is shown that at some point, the zeros become nonminimum-phase which can severely limit the control performance.

We have applied Kwakernaak's frequency minimax approach for the robust control of flexible structures. This method leads to a nonlinear problem and numerical solutions are necessary, but may not be easily obtained. To facilitate the numerical search for the optimal stabilizing controller, we have proposed a procedure which always converges to the stable solution. It is our experience that controllers obtained with the minimax approach have a better robustness than state-variable optimal controllers.

We have also considered the problem of controlling a class of systems characterized by interlaced patterns of poles and zeros on the jω-axis. Because of the irregularities in the pole-zero patterns, the control problem is not an easy task. In fact, we were unable to obtain stable designs with the classical compensation techniques. For the class of systems in consideration, we have developed the concept of generalized lead-lag compensation. This method produces low-order and robust controllers. An important application of the proposed technique is when exact actuator/sensor collocation is not realizable.

In the last part of our work, we have investigated the advantages offered by a multi-sensor design. We have shown that the system robustness can be improved with optimally placed sensors, and derived an optimal sensor placement algorithm for robust control design. The approach is based on eigenstructure assignment and also uses the model dependency on the sensor locations.

It would be of interest to seek an equivalent robust optimal sensor placement in the frequency domain. This brings out the more general problem of establishing a relationship between the condition number of the eigenvector matrix (time-domain measure of robustness) and the matrix-norm stability margins of the frequency domain.

Another direction for future research is to pursue investigating the MIMO control of flexible structures. For truly large flexible structures, a MIMO design is necessary. However, a single centralized MIMO controller may not be practical. Thus, a decentralized approach has to be taken. We mention that the multi-output procedure described in chapter IV can be readily applied for a robust optimal actuator placement in the multi-input case (dual problem). Therefore, the procedure may be generalized to synthesize a robust decentralized control methodology. The corresponding local low-order controllers may be designed with robust optimal

actuator/sensor placement. Then, the stability of the whole interconnected control logic should be assessed. The type of sensors needed and the matching of appropriate sensors with actuators should be investigated. It is also important to minimize the number of actuators and sensors.

REFERENCES

[1] Balas, M.J., "Trends in large space structures control theory: Fondest hopes, wildest dreams", IEEE Transactions on Automatic Control, pp. 522-535, Jun. 1982.

[2] Nurve, G.S. and co-workers, "Dynamics and control of large space structures", Journal of Guidance and Control, pp. 514-526, Sept.-Oct. 1984.

[3] Riley, G., "Saturn V dynamic test vehicle test-analysis correlation", the Boeing Co., Huntsville, Ala., Rept. d5-15722, Nov. 1967

[4] Arthurs, T.D., "Structural Dynamics", Aeronautics and Astronautics, Vol. 17 pp. 95-97, Dec. 1979.

[5] "ACOSS Six (active control of space structures)", Charles Stark Draper Laboratory, Cambridge, Mass., RADC-TR-80-377, Interium Report, Jan. 1981.

[6] Juang, J.N.; Wu, Y.W., " Control of large flexible space structures using pole-placement techniques", Journal of Guidance and Control, pp. 298-303, 1981.

[7] Curtain, R.F., "Pole assignment for distributed systems by finite dimensional control", Automatica, pp. 57-67, 1985.

[8] Meirovitch, L.; Burnh, H., "Robustness of the independent modal-space control method", Journal of Guidance and Control, Jan.-Feb. 1983.

[9] Kabamba, P.T.; Longman, R.W., "An integrated approach to optimal reduced-order control method", The 3rd VPI and SU/AIAA Symposium on Dynamics and Control of Large Flexible Structures, 1981.

[10] Sundararajan, N.V. and co-workers, "Robust controller synthesis for a large flexible space antenna", Journal of Guidance and Control, Mar.-Apr. 1987.

[11] Breakwell, J.A., "Optimal feedback slewing of flexible spacecraft", Journal of Guidance and Control, pp. 472-479, Sept.-Oct. 1981.

[12] Rodriguez, G., " Model error estimation for large space systems", Joint Automatic Control Conference, 1980.

[13] Schaechter, D.B., "Adaptive control for large space structures", AIAA Guidance and Control Conference, 1983.

[14] Kaufman, H. and co-workers, "Model reference adaptive control of large structural systems", Journal of Guidance and Control, pp. 112-118, Mar.-Apr. 1983.

[15] Mufti, I.H., "Model reference adaptive control of large structural systems", Journal of Guidance and Control, pp. 507-509, Sept.-oct. 1987.

[16] Balas, M.J., "Enhanced modal control of flexible structures via innovations feedthrough", International Journal of Control, pp. 983-1003, 1980.

[17] Curtain, R.F., "Spectral Systems", International Journal of Control, pp. 657-666, 1984.

[18] Becker, E.B. and co-workers, "Finite elements: An introduction", Prentice-Hall, 1981

[19] Cruz, J.B. and co-workers, "A relationship between sensitivity and stability of multivariable feedback systems", IEEE Transactions on Automatic Control, Feb. 1981.

[20] Martin, G.D., "On the control of flexible mechanical systems", Ph.D. thesis dissertation, Stanford University, 1978.

[21] Cannon, R.; Schmitz E., "Initial experiments on the end point control of a flexible one-link robot", International Journal of Robotics, Vol 3. , 1984.

[22] Horowitz, I.; Gera, A., "Optimization of the loop transfer function", International Journal of Control, pp. 389-398, 1980.

[23] Zames, G.; Francis, B.A., "on H^{∞} optimal sensitivity theory for SISO feedback systems", IEEE Transactions on Automatic Control, Jan. 1984.

[24] Kwakernaak, H., "Minimax frequency domain performance and robustness optimization of linear systems, IEEE Transactions on Automatic Control, October 1985.

[25] Kwakernaak, H., "A polynomial approach to minimax frequency-domain optimization of multivariable feedback systems", International Journal of Control, pp. 117-156.

[26] Schnabel, R.; Dennis, J.E., "Numerical methods for unconstrained optimization and nonlinear equations", Prentice-Hall, 1983.

[27] Kimura, H.; "Robust stabilizability for a class of transfer functions"; IEEE Transactions on Automatic Control, Sept. 1984.

[28] Franklin, G.F.; Powel, J.D., Emami-Naeini, "Feedback control of dynamic systems", Addison-Wesley, 1986.

[29] Ryan E.P.; Ichikawa, A., "Sensor and controller location problems for distributed parameter systems", Automatica, p.347, 1979.